IFUM-949-FT
Nikhef-2010-001
ITP-UU-10/03
ITFA-2010-01

Heavy quarks in deep-inelastic scattering

Stefano Forte[1,2], Eric Laenen[3], Paolo Nason[4] and Juan Rojo[2]

[1] *Dipartimento di Fisica, Università di Milano and*
[2] *INFN, Sezione di Milano,*
Via Celoria 16, I-20133 Milano, Italy
[3] *ITFA, University of Amsterdam, Valckenierstraat 65, 1018 XE Amsterdam,*
ITF, Utrecht University, Leuvenlaan 4, 3584 CE Utrecht and
Nikhef Theory Group, Science Park 105, 1098 XG Amsterdam, The Netherlands
[4] *INFN, Sezione di Milano-Bicocca,*
Piazza della Scienza 3, I-20126 Milano, Italy

Abstract:

We discuss a general framework for the inclusion of heavy quark mass contributions to deep-inelastic structure functions and their perturbative matching to structure functions computed in variable–mass schemes. Our approach is based on the so–called FONLL method, previously introduced and applied to heavy quark hadroproduction and photoproduction. We define our framework, provide expressions up to second order in the strong coupling, and use them to construct matched expressions for structure functions up to NNLO. After checking explicitly the consistency of our results, we perform a study of the phenomenological impact of heavy quark terms, and compare results obtained at various perturbative orders, and with various prescriptions for the treatment of subleading terms, specifically those related to threshold behaviour. We also consider the heavy quark structure function $F_{2\,c}$ and discuss issues related to the presence of mass singularities in their coefficient functions.

Contents

1 Introduction

Interest in the inclusion of heavy flavour contributions to deep–inelastic electroproduction structure functions was recently revived by the discovery [1] that mass-suppressed terms in global parton fits can affect predictions for the total W and Z production at the LHC by almost 10 %. Indeed, until very recently, many global studies of parton distributions (PDFs, henceforth) were performed assuming heavy quarks to decouple from the structure functions for $Q^2 < m_h^2$, but to be massless when $Q^2 > m_h^2$, despite the availability of more refined approaches where contributions with full mass dependence are consistently taken into account.

A technique for the inclusion of heavy mass-suppressed contributions to structure functions was developed long ago [2,3], based upon a renormalization scheme with explicit heavy quark decoupling [4]. Several variants of this method (usually called ACOT) were subsequently proposed, such as S-ACOT [5] and ACOT-χ [6, 7]. However, the ACOT method was first used for an actual global parton fit only recently, in Refs. [1, 7]. An alternative method (sometimes called TR) has also been advocated [8–10], and used for parton fits [11–13]. Recently, however, the methods used by the CTEQ [1] and MSTW [14] groups for their current parton fits, based respectively on the ACOT [2, 3] and TR [8–10] procedures, have adopted at least in part a common framework: they have been compared recently in Refs. [15, 16], thereby elucidating differences and common aspects.

A somewhat different technique for the inclusion of heavy quark effects, the so called FONLL method, was introduced in Ref. [17] in the context of hadroproduction of heavy quarks. The FONLL method only relies on standard QCD factorization and calculations with massive quarks in the decoupling scheme of Ref. [4] and with massless quarks in the $\overline{\rm MS}$ scheme. The name FONLL is motivated by the fact that the method was originally used to combine a fixed (second) order calculation with a next-to-leading log one; however, the method is entirely general, and it can be used to combine consistently a fixed order with a resummed calculation to any order of either.

It is the purpose of this paper to present the application of the FONLL scheme to deep–inelastic structure functions. We shall see that, thanks to its simplicity, the method actually provides a framework for understanding differences between other existing approaches, and for a study of the effect of different choices in the inclusion of subleading terms. We shall use this scheme to perform detailed studies of the phenomenological impact of the treatment of heavy quarks up to NNLO, and of the ambiguities involved in the procedure.

In section 2 we will describe in detail the theory of the FONLL method for structure functions. In section 3 we will provide explicit expressions up to NNLO, and discuss issues related to perturbative ordering. In section 4 we shall compare the structure functions determined with different heavy quark matching procedures at various orders, and with various treatments of threshold subleading terms. Finally, in section 5 we shall discuss issues related to the presence of mass singularities in the definition of the heavy quark structure functions $F_{2\,c}$ and $F_{2\,b}$. For ease of reference and for definiteness, the complete explicit FONLL expressions for the structure function F_2 are collected in an Appendix.

2 The FONLL method in deep-inelastic scattering

The basic problem in the treatment of heavy quarks in a QCD process stems from the fact that QCD calculations are usually performed in a decoupling scheme [4], rather than in the $\overline{\rm MS}$ scheme. Indeed, in the standard $\overline{\rm MS}$ scheme, heavy quarks contributions are present at all scales: for instance, the β function depends on n_f with $n_f = 6$ at all scales. In a decoupling scheme, instead, in the computation of a process characterized by the hard scale Q^2 all quarks with mass $m_q^2 > Q^2$ ("heavy", henceforth) are not treated in the $\overline{\rm MS}$ scheme. Rather, 'heavy flavour graphs' are subtracted at zero momentum.[1] The important consequence of this definition is that heavy quarks decouple for scales much lower than the heavy quark mass. This implies that the GLAP evolution equations, and the running of α_s are identical to those which one would get in the $\overline{\rm MS}$ scheme, but with n_f equal to the number of light flavours, $n_f = n_l$. If for $Q^2 < m_h^2$ one neglects all terms suppressed by powers of Q^2/m_h^2, one obtains a so–called zero–mass scheme, where all quarks are treated as massless, but heavy quarks are absent at $Q^2 \leq m_h^2$. This scheme can be combined with the usual $\overline{\rm MS}$ scheme for $n_l + 1$ flavours, including the heavy quark, when $Q^2 \geq m_h^2$; if terms suppressed by powers of m_h^2/Q^2 are neglected throughout this yields the so called zero–mass variable–flavour number scheme (ZMVFN from now on) of Ref. [3].[2]

The ZMVFN scheme is not accurate near the threshold region, where $\frac{m_h^2}{Q^2} \sim 1$. The problem in this region is easily remedied by simply using the decoupling scheme with $n_f = n_l$, but retaining explicitly the full dependence on the heavy quark mass in the computation of hard cross sections. This way of computing however looses accuracy in comparison to the previous ZMVFN when $Q^2 \gg m_h^2$ so that $L \equiv \ln Q^2/m_h^2 \gg 1$, because, in the decoupling scheme with $n_f = n_l$, these large logs are only included to fixed order in α_s while in the ZMVFN scheme they are resummed to all orders.

Heavy quark schemes are all based on the idea of matching these two different ways of calculating, each of which is more accurate in some kinematic region. The basic idea in the ACOT [3] scheme is to retain explicitly the mass dependence in Wilson coefficients of the ZMVFN scheme calculation (based on the massive quark factorization theorem [2]), while the basic idea in the TR [8, 9] scheme is to require continuity of physical observables in the threshold region, where one switches between the decoupling scheme and the massless calculation with $n_f = n_l + 1$ flavours. In both cases, the matching conditions ensue from the requirement that computations of the same observable within different renormalization schemes give the same answer within the respective accuracy.

The FONLL scheme is instead simply based on the idea of combining the decoupling scheme computation with the ZMVFN computation, and subtracting double counting terms between the two order by order in an expansion in powers of α_s and L. Effectively,

[1] Here 'heavy flavour graphs' are defined [4] (recursively) as either graphs which contain a heavy flavour line, or counterterms to heavy flavour graphs.

[2] Note that here and henceforth we call "variable–flavour number" scheme (VFN, and thus also ZMVFN) a scheme where all large Q^2 logs are resummed, so in particular, when $Q^2 >> m_h^2$ all $\ln \frac{Q^2}{m_h^2}$ terms are resummed. In contrast, in some previous references, VFN or ZMVFN is used to denote schemes in which $\ln \frac{Q^2}{m_h^2}$ are not resummed to all orders: in particular in Ref. [18] VFN denotes the scheme in which logs are not resummed, while that in which logs are resummed is called "PDF". In Ref. [19] ZMVFN is used despite the fact that $\ln \frac{Q^2}{m_h^2}$ are never resummed to all orders in this reference [20].

this means that for $Q^2 > m_h^2$ one performs the calculation in the massless scheme, but then one replaces all terms whose mass-dependence is known with their exact massive expression. This can then be done to any desired order.

2.1 FONLL expressions for DIS structure functions

Let us now see explicitly how the FONLL scheme works in the case of a generic deep-inelastic structure function $F(x,Q^2)$: in Sects. 3-4 we shall specifically discuss both F_2 and F_L, but for the time being the distinction is irrelevant, so we will refer to a generic structure function F. For the rest of the paper we will assume n_l light flavours, with a single heavy flavour of mass $m_h = m$. In Sec. 4, when discussing phenomenological implications, we will study specifically the case of charm.

The expression of $F(x,Q^2)$ in the fully massless scheme, which is accurate when $W \gg 4m^2$, with $W \equiv \sqrt{Q^2(1-x)/x}$, is factorized in terms of PDFs[3]

$$F^{(n_l+1)}(x,Q^2) = x\int_x^1 \frac{dy}{y} \sum_{i=q,\bar{q},h,\bar{h},g} C_i^{(n_l+1)}\left(\frac{x}{y},\alpha_s^{(n_l+1)}(Q^2)\right) f_i^{(n_l+1)}(y,Q^2), \qquad (1)$$

where q is any light quark, h is the heavy quark, and n_l+1 is the total number of flavours. In this expressions, the PDFs include the heavy flavour as a light parton, and the strong coupling $\alpha_s^{(n)}$ and the PDFs $f_i^{(n)}$ satisfy standard GLAP equations with $n_f = n_l + 1$. Henceforth, we shall refer to Eq. (1) as the determination of $F(x,Q^2)$ in the massless scheme.

The expression of $F(x,Q^2)$ in the decoupling scheme with $n_f = n_l$, which is accurate when $W \approx 4m^2$, is instead given by

$$F^{(n_l)}(x,Q^2) = x\int_x^1 \frac{dy}{y} \sum_{i=q,\bar{q},g} C_i^{(n_l)}\left(\frac{x}{y},\frac{Q^2}{m^2},\alpha_s^{(n_l)}(Q^2)\right) f_i^{(n_l)}(y,Q^2). \qquad (2)$$

The coefficient functions are computed fully retaining the mass dependence, while now $\alpha_s^{(n_l)}$ and $f_i^{(n_l)}(y,Q^2)$ obey standard $\overline{\rm MS}$ evolution equations with n_l flavours. When $W^2 \ll 4m^2$ the heavy quark mass dependence drops out of the coefficient functions $C_i^{(n_l)}$, which then reduce to the standard massless $\overline{\rm MS}$ coefficient functions with n_l flavours. Henceforth, we shall refer to Eq. (2) as the determination of $F(x,Q^2)$ in the massive scheme.

In order to carry out the FONLL procedure, we need to express the decoupling scheme cross section, Eq. (2) in terms of $\alpha_s^{(n_l+1)}$ and $f_i^{(n_l+1)}$ for $i \neq h,\bar{h}$. The coupling constant and PDFs are related in the two schemes by equations of the form

$$\alpha_s^{(n_l+1)}(Q^2) = \alpha_s^{(n_l)}(Q^2) + \sum_{i=2}^{\infty} c_i(L) \times \left(\alpha_s^{(n_l)}(m^2)\right)^i , \qquad (3)$$

$$f_i^{(n_l+1)}(x,Q^2) = \int_x^1 \frac{dy}{y} \sum_{j=q,\bar{q},g} K_{ij}\left(\frac{x}{y},L,\alpha_s^{(n_l)}(Q^2)\right) f_j^{(n_l)}(y,Q^2) , \qquad (4)$$

[3]Note that we define PDFs $f(x)$ in such a way that $xf(x)$ is a momentum distribution; a different definition such that $f(x)$ is the momentum distribution itself, which differs from our own by a factor of x, has also been sometimes used (see e.g. Ref. [21]).

where

$$L \equiv \log Q^2/m^2. \tag{5}$$

The coefficients $c_i(L)$ are polynomials in L, and the functions K_{ij} can be expressed as an expansion in powers of α_s, with coefficients that are polynomials in L.

The first $2n_l + 1$ equations in Eq. (4) relate the light quark and gluon PDFs in the two schemes, and can be inverted to express the massive–scheme PDFs in terms of the massless-scheme ones. The last two equations in Eq. (4) express heavy quark PDFs in terms of the light flavour ones, under the assumption that the heavy flavour PDF is generated perturbatively. A possible intrinsic heavy flavour contribution [22, 23] could be added as a separate contribution on the right-hand side of Eq. (4) for $i = h,\ \bar{h}$.

Inverting Eqs. (3-4) and substituting in Eq. (2), one can obtain an expression of $F^{(n_l)}(x, Q^2)$ in terms of $\alpha_s^{(n_l+1)}$ and $f^{(n_l+1)}$:

$$F^{(n_l)}(x, Q^2) = x \int_x^1 \frac{dy}{y} \sum_{i=q,\bar{q},g} B_i \left(\frac{x}{y}, \frac{Q^2}{m^2}, \alpha_s^{(n_l+1)}(Q^2) \right) f_i^{(n_l+1)}(y, Q^2), \tag{6}$$

where the coefficient functions B_i are such that substituting the matching relations Eqs. (3-4) in Eq.(6) one gets back the original expression Eq. (2). We can thus use for $F^{(n_l)}$ the expression given in Eq. (6), and avoid any further reference to $\alpha_s^{(n_l)}$ and $f_i^{(n_l)}$: from now on, we shall use Eq. (6) as the determination of F in the massive scheme.

In order to match the two expressions for F in the massless scheme, Eq. (1), and in the massive scheme, Eq. (6), we now work out their perturbative expansion. Using GLAP evolution in the absence of intrinsic heavy quark contributions, the heavy quark PDFs $f_h^{(n)}$, $f_{\bar{h}}^{(n)}$ at the scale Q^2 which appear in the massless–scheme expression Eq. (1) can be determined in terms of the light-quark PDFs, $f_i^{(n_l)}$ with $i \neq h,\ \bar{h}$ at the scale m, convoluted with coefficient functions which can be expressed as a power series in $\alpha_s^{(n_l)}(m)$, with coefficients that are polynomials in L, or, alternatively, in terms of the light-quark parton distributions $f_i^{(n_l+1)}$ at the scale Q^2 convoluted with coefficient functions expressed as a power series in $\alpha_s^{(n_l+1)}(Q^2)$, again with (different) coefficients that are polynomials in L.

Thus, the massless-scheme expression Eq. (1) may be written entirely in terms of light-quark PDFs:

$$F^{(n_l+1)}(x, Q^2) = x \int_x^1 \frac{dy}{y} \sum_{i=q,\bar{q},g} A_i^{(n_l+1)} \left(\frac{x}{y}, L, \alpha_s^{(n_l+1)}(Q^2) \right) f_i^{(n_l+1)}(y, Q^2), \tag{7}$$

where the $A_i^{(n_l+1)}$ coefficient functions are given by a perturbative expansion of the form

$$A_i^{(n_l+1)} \left(z, L, \alpha_s^{(n_l+1)}(Q^2) \right) = \sum_{p=0}^{N} \left(\alpha_s^{(n_l+1)}(Q^2) \right)^p \sum_{k=0}^{\infty} A_i^{p,k}(z) \left(\alpha_s^{(n_l+1)}(Q^2) L \right)^k, \tag{8}$$

where at leading order $N = 0$, and at N^{k}LO $N = k$.

On the other hand, the massive-scheme expression Eq. (6) is also written in terms of the light quark PDFs, with coefficient functions B_i which admit a fixed order expansion

of the form

$$B_i\left(z,\frac{Q^2}{m^2},\alpha_s^{(n_l+1)}(Q^2)\right)=\sum_{p=0}^{P}\left(\frac{\alpha_s^{(n)}(Q^2)}{2\pi}\right)^p B_i^p\left(z,\frac{Q^2}{m^2}\right), \tag{9}$$

where P is the order of the expansion needed to reach the desired accuracy. It follows that the sum $B_i^{(0),\,p}$ of all contributions to the massive-scheme expression Eq. (9) which do not vanish when $Q^2 \gg m^2$ must also be present in the massless-scheme result, i.e. they must correspond to the logarithmic and constant terms in Eq. (8). Namely, to p–th order in $\alpha_s^{(n_l+1)}(Q^2)$

$$B_i^{(0),\,p}\left(x,\frac{Q^2}{m^2}\right)\equiv\sum_{k=0}^{p}A_i^{p-k,k}(x)L^k, \tag{10}$$

where we denote by $B_i^{(0),\,p}$ the massless limit of B_i^p, in the sense that

$$\lim_{m\to 0}\left[B_i^p\left(x,\frac{Q^2}{m^2}\right)-B_i^{(0),\,p}\left(x,\frac{Q^2}{m^2}\right)\right]=0. \tag{11}$$

In other words, $B_i^{(0),\,p}$ is obtained from B_i^p by retaining all logarithmic and constant terms, and dropping all terms suppressed by powers of m/Q.

The FONLL method can be simply stated as follows: in the massless-scheme expression Eq. (7) one replaces all contributions to the expansion (8) of the coefficient functions $A_i^{(n_l+1)}\left(z,L,\alpha_s^{(n_l+1)}(Q^2)\right)$ which appear in $B_i^{(0),\,p}\left(x,\frac{Q^2}{m^2}\right)$, Eq. (10), with their fully massive expression $B_i^p\left(x,\frac{Q^2}{m^2}\right)$ from Eq. (6). In this way, all the mass suppressed effects that are not present in Eq. (1) but are known from Eq. (2) are included.

In order to do this in a systematic way, we define thus the massless limit of the massive-scheme expression Eq.(6), namely

$$F^{(n_l,\,0)}(x,Q^2)=x\int_x^1\frac{dy}{y}\sum_{i=q,\bar{q},g}B_i^{(0)}\left(\frac{x}{y},\frac{Q^2}{m^2},\alpha_s^{(n_l+1)}(Q^2)\right)f_i^{(n_l+1)}(y,Q^2), \tag{12}$$

where

$$B_i^{(0)}\left(z,\frac{Q^2}{m^2},\alpha_s^{(n_l+1)}(Q^2)\right)=\sum_{p=0}^{P}\left(\alpha_s^{(n_l+1)}(Q^2)\right)^m B_i^{(0),\,p}\left(z,\frac{Q^2}{m^2}\right), \tag{13}$$

with $B_i^{(0),\,p}$ given by Eq. (10), and the sum over p consistently performed including all terms up to the order P in $\alpha_s^{(n_l+1)}(Q^2)$ to which the massive-scheme expression has been determined.

The FONLL approximation for F_2 is then given by

$$F^{\rm FONLL}(x,Q^2)=F^{(d)}(x,Q^2)+F^{(n_l)}(x,Q^2), \tag{14}$$

$$F^{(d)}(x,Q^2)\equiv\left[F^{(n_l+1)}(x,Q^2)-F^{(n_l,\,0)}(x,Q^2)\right] \tag{15}$$

where $F^{(n_l)}$ is the massive-scheme expression Eq. (6), and the "difference" contribution Eq. (15) is constructed out of the massless-scheme expression $F^{(n_l+1)}$ Eq. (7), and the massless limit $F^{(n_l,\,0)}$ Eq. (12) of the massive-scheme expression.

Because of Eq. (11), when $Q^2 \gg m^2$ the FONLL expression reduces to the massless-scheme one $F^{(n_l+1)}$. When instead $Q^2 \approx m^2$ the FONLL expressions differ from the massive-scheme one $F^{(n_l)}$ through the "difference" term $F^{(d)}$ Eq. (15), which is however subleading in $\alpha_s(Q^2)$. Note that in the FONLL scheme continuity does not play a role in the matching conditions: at NLO continuity ensues accidentally from the matching conditions, but at higher orders subleading discontinuities may arise.

When $Q^2 < m^2$, but $W^2 > 4m^2$ i.e. above the threshold for heavy quark production there are various options. A simple possibility is to just use the massive scheme result Eq. (6). It is easy to see that this amounts to replacing the "difference" term in Eq. (14) by

$$F^{(d')}(x,Q^2) \equiv \left[F^{\rm ZMVFN}(x,Q^2) - \Theta(Q^2-m^2)F^{(n_l,0)}(x,Q^2)\right] \tag{16}$$

where $F^{\rm ZMVFN}(x,Q^2)$ denotes the massless calculation with $n_f = n_l + 1$ when $Q^2 > m^2$, and with $n_f = n_l$ when $Q^2 < m^2$: this is identical to Eq. (14) for $Q^2 > m^2$, and it reduces to the massive calculation for $Q^2 < m^2$ because the term in square brackets vanishes there. Of course, when $Q^2 \ll m^2$ and $W^2 \ll 4m^2$ the massive calculation in turn coincides with the massless calculation with $n_f = n_l$, so one recovers the same result as the ZMVFN in this region. However, if one only wishes to use the result at scales Q^2 which are never much lower than m^2, a simpler option may be to just use Eq. (14) everywhere. Then, when $Q^2 < m^2$ but $W^2 > 4m^2$ the term in square brackets will contain some small contributions in the $n_f = n_l + 1$ scheme evolved backwards below the heavy quark threshold.

The FONLL formula Eq. (14) may look similar to a prescription suggested in Ref. [18], and then further discussed in Ref. [24] (in particular Eq. (5) of the latter), sometimes referred to as the BMSN prescription, which is also based on the idea of combining computations performed in schemes which differ in the number of active flavours. However, in the BMSN method the issue of using PDF defined in a single factorization scheme in all terms is not addressed (unlike in FONLL, where it is accomplished expressing everything, Eq. (7), in terms of $\alpha_s^{(n_l+1)}$ and $f^{(n_l+1)}$). This leads to inconsistent results beyond $\mathcal{O}(\alpha_s)$, as stated in Ref. [24], where it is argued that the inconsistency is however numerically small in practice. Also, contributions proportional to the light or heavy quark electric charge are not easily separated in the BSMN method, again leading to (possibly small [24]) inconsistencies beyond $\mathcal{O}(\alpha_s)$, unlike in FONLL where this separation can be treated in a fully consistent way as we will do explicitly to $\mathcal{O}(\alpha_s^2)$ in Sect. 3.2 below. As for the comparison of FONLL to the ACOT and TR schemes, we will come back to it in the end of Sect. 3.3, after fully specifying the FONLL scheme up to $\mathcal{O}(\alpha_s^2)$.

Finally, it should be observed that near threshold the $F^{(d)}$ term Eq. (15), though subleading, could in practice be non–negligible, and it does not provide any information because it contains higher–order logarithmic contributions in a region in which L is not large. In practice, it may thus be convenient to suppress this term through a suitable kinematic factor when Q is near m_h, which is allowed without modifying the accuracy of the calculation because this term is subleading, as we shall discuss in the next section.

2.2 Mismatch in accuracy

In order for Eq. (14) and (15) to work properly, it is necessary to determine $F^{(n_l+1)}$ with an accuracy which is at least as high as that used in the computation of $F^{(n_l)}$. Only in

this case, in fact, in the difference expression Eq. (15) we are subtracting terms that are actually present in $F^{(n_l+1)}$.

However, it is possible to generalize Eq. (15) in such a way that it can still be used even when $F^{(n_l)}$ is known with higher accuracy than $F^{(n_l+1)}$. For this purpose, it is sufficient to retain in $F^{(n_l,0)}$ in (15) only those terms that are also present in $F^{(n_l+1)}$. In this case, it is no longer true that when $Q^2 \gg m^2$ the FONLL expression reduces to the massless scheme one $F^{(n_l+1)}$ up to mass suppressed terms only. In fact, $F^{(n_l,0)}$ in (15) and $F^{(n_l)}$ in (14) no longer cancel in this limit, since some terms have been excluded from $F^{(n_l,0)}$. It is however still true that the FONLL reduces to the massless scheme one $F^{(n_l+1)}$ up to mass suppressed terms and terms of higher order in $\mathcal{O}(\alpha_s)$. Further on, we will illustrate an application of this approach to the charm structure function, where $F_c^{(n_l+1)}$ is evaluated at NLO, and $F_c^{(n_l,0)}$ is evaluated at order $\mathcal{O}(\alpha_s^2)$.

2.3 The heavy quark threshold

As already stated, when $Q \approx m$ the $F^{(d)}$ term becomes totally unreliable, since it contains higher–order contributions enhanced by powers of L, in a region in which L is not large. It may then be advisable to suppress $F^{(d)}$ Eq. (15) in the threshold region. Because $F^{(d)}$ is formally subleading, this of course does not change the nominal accuracy of the calculation, but it may in practice improve the perturbative stability and smoothness of the result.

This suppression can be obtained in various ways. Two classes of possibilities which have been considered in previous studies consist of introducing a threshold factor or a rescaling variable. In the former case, one replaces $F_2^{(d)}$ Eq. (15) with

$$F^{(d,\,th)}(x,Q^2) = f_{\rm thr}(x,Q^2) F^{(d)}(x,Q^2), \tag{17}$$

where $f_{\rm thr}$ is such that $F^{(d,\,th)}(x,Q^2)$ only differs from $F^{(d)}(x,Q^2)$ by terms that are power–suppressed for large Q^2, namely

$$f_{\rm thr}(x,Q^2) = 1 + \mathcal{O}\left(\frac{m^2}{Q^2}\right) \tag{18}$$

but it enforces vanishing of $F^{(d,\,th)}(x,Q^2)$ below the threshold at $Q^2 = m^2$. A suitable choice is

$$f_{\rm thr}(x,Q^2) = \Theta(Q^2-m^2)\left(1-\frac{Q^2}{m^2}\right)^2, \tag{19}$$

where the factor in brackets ensure that $f_{\rm thr}(x,Q^2)$ and its first derivative with respect to Q^2 are continuous at $Q^2 = m^2$.

When using a rescaling variable, one instead replaces in all convolutions which enter the expression for $F^{(d)}$ the variable x with a new rescaling variable $\chi(x,Q^2)$, so that the factorized expression of all structure functions is now given by

$$F^{(\chi)}(x,Q^2) = x\int_{\chi(x,Q^2)}^1 \frac{dy}{y} C\left(\frac{\chi(x,Q^2)}{y},\alpha(Q^2)\right) f(y,Q^2), \tag{20}$$

where the rescaling variable $\chi(x,Q^2)$ is chosen in such a way that again $F^{(d,\,\chi)}(x,Q^2)$ only differs from $F^{(d)}(x,Q^2)$ by power suppressed terms, namely

$$\chi(x,Q^2) = x + \mathcal{O}\left(\frac{m^2}{Q^2}\right), \tag{21}$$

but it is such that, viewed as a function of x, $F^{(d,\,th)}(x,Q^2)$ only has support above threshold. The threshold can be set at the physical production value $W^2 = m^2$ by choosing

$$\chi = x\left(1 + \frac{4m^2}{Q^2}\right). \tag{22}$$

This choice was adopted in Ref. [6,7], and the ACOT method supplemented by it is called the ACOT-χ prescription; it is used among others in the recent CTEQ parton fits [1].[4]

A generalization of the χ variable was introduced in Ref. [26], by defining a one-parameter family of variables which interpolate between x and χ, but all of which set the threshold at the physical value. In fact, it was argued in Ref. [15] that a full treatment of heavy quark threshold such as ACOT or the FONLL method discussed here could be well–approximated by simply using the ZMVFN, but with x replaced by a suitable fine–tuned χ–like variable. Be that as it may, we note that within the FONLL (or ACOT) method there is no conceptual advantage in introducing a suppression at the physical threshold W^2 over a suppression at $Q^2 = m^2$, given that for most of the interesting kinematic region the physical threshold correspond to values of Q^2 which are lower than m^2, and where thus the massive expression is being used anyway.

In Ref. [17], which dealt with hadroproduction of heavy quarks, yet another form of a suppression factor was proposed, based on the transverse momentum of the heavy quark pair. We remark here that there is no straightforward generalization of the χ-scaling prescription to the hadroproduction case.

All these threshold modifications of higher order terms, being subleading, can neither be justified nor be excluded a priori. Their purpose is to mimic in a phenomenological way the effect of finite mass effects not included in the calculation. They can thus be validated to a certain extent by comparing results obtained using these prescriptions with exact results when the latter are known, though of course this does not prove that their effect will be the same or similar when the exact result is not known. We will perform this validation in section 4.2 below.

3 Implementation of the FONLL method

We shall now work out explicitly the FONLL prescription Eq. (14) up to $\mathcal{O}(\alpha_s^2)$. We will discuss separately the contributions to the structure function in which the virtual photon couples to the heavy quark only ("heavy" structure function F_h) and the rest. The basic ingredient in the FONLL construction is the scheme change of Eqs. (3-4). We will first work this out up to order α_s^2, then use it to construct up to the same order the various contributions to the FONLL expression of Eq. (14). We will then combine these

[4] Note that a slightly different definition of rescaling is also possible, whereby one simply lets

$$F^{(d,\,\chi)} = F^{(d)}(\chi(x,Q^2),Q^2). \tag{23}$$

This definition, which differs by the above one by a factor $\frac{\chi}{x}$, has been for instance discussed in Ref. [11]; however, the definition Eq. (20) is used by CTEQ [25].

contributions into expressions for the structure functions. Throughout this section we will discuss a generic structure function $F(x,Q^2)$, and all formulae will be valid for both F_2 and F_L unless otherwise stated.

It is important at this point to recall that the meaning of "NNLO" in this context is partly a matter of convention: one may use an absolute definition, where LO is $\mathcal{O}(1)$, NLO the $\mathcal{O}(\alpha_s)$ and so on, or a relative definition, in which the LO is defined as the first non–vanishing order, or a combination of the above according to the observable which is being considered. Various options which are relevant for PDF determination up to NNLO will be discussed in Sec. 3.3. Finally, we will provide explicit numerical checks of the consistency of our procedure in the various cases.

3.1 Scheme change

First of all let us discuss the details of the change between the scheme with n_l flavours (massive scheme) and that with $n_f = n_l + 1$ flavours (massless scheme). For future convenience, we define

$$a_s(Q^2) \equiv \frac{\alpha_s(Q^2)}{2\pi}; \quad \beta_0 \equiv 2\pi b_0, \tag{24}$$

with

$$b_0 = \frac{33 - 2n_f}{12\pi} \ . \tag{25}$$

The running of the coupling with n_f flavours to lowest nontrivial order is given by

$$\alpha_s(Q^2) = \alpha_s(m^2) - b_0 \log\frac{Q^2}{m^2}\alpha_s^2 + \mathcal{O}(\alpha_s^3). \tag{26}$$

3.1.1 Matching

At a given value of Q^2 the relation between the coupling constant in the massless and massive schemes, Eq. (3), reads

$$a_s^{(n_l+1)}(Q^2) = a_s^{(n_l)}(Q^2) + \frac{2T_R}{3}a_s^2 L + \mathcal{O}(\alpha_s^3), \tag{27}$$

which immediately implies that the two schemes coincide when the scale is equal to the heavy quark mass:

$$a_s^{(n_l+1)}(m) = a_s^{(n_l)}(m) + \mathcal{O}(\alpha_s^3). \tag{28}$$

Since all coefficient functions at NNLO are at most of order $\mathcal{O}(\alpha_s^2)$, we will not need terms of order $\mathcal{O}(\alpha_s^3)$ in the matching condition for α_s.

The relation between parton distributions, Eq. (4), for light partons in the two schemes at $Q^2 = m^2$ is also trivial up to order α_s,

$$f_i^{(n_l+1)}(x,m^2) = f_i^{(n_l)}(x,m^2) + \mathcal{O}(\alpha_s^2), \tag{29}$$

but it becomes nontrivial starting at $\mathcal{O}(\alpha_s^2)$, because at this order contributions from heavy quark loops arise, which can thus contribute to the renormalization of light flavours and gluons in the massless scheme where $n_f = n_l + 1$. We have thus

$$f_i^{(n_l+1)}(x,m^2) = f_i^{(n_l)}(x,m^2) + a_s^2\int\frac{dz}{z}\sum_j K_{ij}(z) f_j^{(n_l)}\left(\frac{x}{z},m^2\right) + \mathcal{O}(\alpha_s^3), \tag{30}$$

where the indices i, j take the values q, $\bar{q}$, g, and the functions K_{qq}, K_{gq} and K_{gg} were computed in Ref. [18], where they are respectively given in Eqs. (B4, B5, B7). On the other hand, in the absence of an intrinsic heavy quark contribution, the matching conditions Eq. (4), in the case of the heavy quark distribution are

$$f_h^{(n_l+1)}(x,m^2) = f_{\bar{h}}^{(n_l+1)}(x,m^2) = \mathcal{O}(\alpha_s^2). \tag{31}$$

As already mentioned, the coefficient functions C_i start at order one only in the case of the light quark contribution to F_2 (in the absence of intrinsic heavy quark contributions). Therefore, up to order α_s^2, the only nontrivial contribution to matching Eq. (30) is due to light quarks: gluon contributions to structure functions start at $\mathcal{O}(\alpha_s)$, thus the contribution from K_{gq} and K_{gg} to structure functions only start at $\mathcal{O}(\alpha_s^3)$. Therefore, in this paper we will only use Eq. (30) for light quarks, in the form

$$f_q^{(n_l)}(x,m^2) = f_q^{(n_l+1)}(x,m^2) - a_s^2 \int \frac{dz}{z} K_{qq}(z) f_q^{(n_l+1)}\left(\frac{x}{z}, m^2\right) + \mathcal{O}(\alpha_s^3), \tag{32}$$

with[5]

$$K_{qq} = C_F T_R \left[\frac{1+z^2}{1-z} \left(\frac{1}{6}\log^2 z + \frac{5}{9}\log z + \frac{28}{27} \right) + (1-z)\left(\frac{2}{3}\log z + \frac{13}{9} \right) \right]_+ . \tag{33}$$

3.1.2 Scale dependence

While the matching condition for parton distributions at the scale $Q^2 = m^2$, Eqs. (30), is sufficient in order to fix the relation between PDFs in the massive and massless schemes, in order to implement the FONLL approximation we need to express the massive-scheme PDFs in terms of the massless-scheme ones at a generic scale Q^2, as required in Eq. (6). The relation at any scale can be obtained from the matching condition Eq. (30) by solving the evolution equation for both $f_i^{(n_l+1)}$ and $f_i^{(n_l)}$ in the respective schemes. Because only the light quark coefficient function starts at $\mathcal{O}(\alpha_s^0)$, up to order α_s^2 matching conditions at $\mathcal{O}(\alpha_s)$ will be sufficient for gluons, while $\mathcal{O}(\alpha_s^2)$ will be required for quarks.

Evolving up to Q^2 Eq. (29) to order α_s gives

$$f_i^{(n_l+1)}(x,Q^2) = f_i^{(n_l)}(x,Q^2) + a_s L \int_x^1 \frac{dz}{z} \sum_j \left[P_{ij}^{(n_l+1),0}(z) - P_{ij}^{(n_l),0}(z) \right] f_j^{(n_l)}\left(\frac{x}{z}, Q^2\right) + \mathcal{O}(\alpha_s^2), \tag{34}$$

where $P_{ij}^0(z)$ are leading–order Altarelli-Parisi splitting functions in the two schemes, and the sum runs over all PDFs. Noting that

$$P_{ij}^{(n_l+1),0}(z) - P_{ij}^{(n_l),0}(z) = -\delta_{ig}\delta_{jg}\frac{2T_R}{3}\delta(1-z). \tag{35}$$

it immediately follows that the relation between gluon distributions at scale Q^2 is

$$f_g^{(n_l+1)}(x,Q^2) = f_g^{(n_l)}(x,Q^2) - a_s L \frac{2T_R}{3} f_g^{(n_l+1)}(x,Q^2) + \mathcal{O}(\alpha_s^2) \tag{36}$$

[5]Note that the expression given here differs by a factor 4 from that obtained setting $\mu = m$ in Eq. (B4) of Ref. [18] because we expand in powers of $\frac{\alpha_s}{2\pi}$ and not $\frac{\alpha_s}{4\pi}$ as in that reference; note also that we have absorbed all distributions into the + prescription.

To order α_s^2 Eq. (34) is modified because the initial condition at $Q^2 = m^2$ becomes Eq. (30), and also because the evolution mismatch receives three further contributions: from the change in running coupling Eq. (27), from the second iteration of the leading–order splitting functions $P_{ij}^{(0)}$, and from the next–to–leading order splitting functions $P_{ij}^{(1)}$. Combining these contributions, the matching condition Eq. (30) becomes

$$\begin{aligned} f_q^{(n_l)}(x,Q^2) &= f_q^{(n_l+1)}(x,Q^2) - a_s^2 \int \frac{dz}{z} K_{qq}(z) f_q^{(n_l+1)}\left(\frac{x}{z}, m^2\right) \\ &- a_s^2 L \int_x^1 \frac{dz}{z} \frac{2T_R}{3} \frac{L}{2} \sum_{j \in q\bar{q}g} P_{qj}^{(n_l),\,0}(z) \times f_j^{(n_l+1)}\left(\frac{x}{z}, Q^2\right) \\ &+ \frac{(a_s L)^2}{2} \frac{2T_R}{3} \int_x^1 \frac{dz}{z} P_{qg}^{(n_l),\,0}(z) f_g^{(n_l+1)}\left(\frac{x}{z}, Q^2\right) \\ &- a_s^2 L \int_x^1 \frac{dz}{z} \sum_{j \in q\bar{q}g} \left[P_{qj}^{(n_l+1),\,1}(z) - P_{qj}^{(n_l),\,1}(z)\right] \times f_j^{(n_l)}\left(\frac{x}{z}, Q^2\right) + \mathcal{O}(\alpha_s^3), \end{aligned} \tag{37}$$

where each line in Eq. (37) corresponds respectively to each of the contributions listed above. Note that, because of Eq. (35), the $\mathcal{O}(\alpha_s)$ correction vanishes for light quarks. Note also that the f_g contribution cancels between the second and third line in Eq. (37). Using the fact that [27]

$$P_{qj}^{(n_l+1),\,1}(z) - P_{qj}^{(n_l),\,1}(z) = -\delta_{jq} \Delta_{qq}(z), \tag{38}$$

with

$$\Delta_{qq}(z) = C_F T_R \left[\frac{1+z^2}{1-z}\left(\frac{2}{3}\log z + \frac{10}{9}\right) + \frac{4}{3}(1-z)\right]_+ \tag{39}$$

we reproduce the result of Ref. [18]:

$$\begin{aligned} f_q^{(n_l)}(x,Q^2) &= f_q^{(n_l+1)}(x,Q^2) - a_s^2 \int \frac{dz}{z} K_{qq}(z,L) f_j^{(n_l+1)}\left(\frac{x}{z}, Q^2\right) \\ K_{qq}(z,L) &= K_{qq}(z) + \frac{L^2}{2} \frac{2T_R}{3} P_{qq}^{(n_l),\,0}(z) - L \Delta_{qq}(z), \end{aligned} \tag{40}$$

with $K_{qq}(z)$ and $\Delta_{qq}(z)$ given respectively by Eqs. (33-39).

3.2 The FONLL approximation up to $\mathcal{O}(\alpha_s^2)$

It is now convenient to separate off explicitly the light and heavy contributions to the generic structure function F and its corresponding coefficient functions C_i:

$$\begin{aligned} F(x,Q^2) &= F_l(x,Q^2) + F_h(x,Q^2); \\ C_i(x,\alpha_s(Q^2)) &= C_{i,\,l}(x,\alpha_s(Q^2)) + C_{i,\,h}(x,\alpha_s(Q^2)) \end{aligned} \tag{41}$$

where we define F_h and $C_{i,\,h}$ as the contributions to F and C_i respectively which are obtained when only the electric charge of the heavy quark is nonzero. Note that therefore, up to $\mathcal{O}(\alpha_s^2)$, in the coefficient functions the label l, h denotes the quark to which the virtual photon couples, whereas the label i denotes the parton that enters the hard scattering

process.[6] The separation of Eq. (41) will be carried through also for the corresponding FONLL expressions (Eqs. (14, 15)), i.e. we will write

$$F_l^{\rm FONLL}(x,Q^2) = F_l^{(n_l)}(x,Q^2) + F_l^{(d)}(x,Q^2), \tag{42}$$

$$F_h^{\rm FONLL}(x,Q^2) = F_h^{(n_l)}(x,Q^2) + F_h^{(d)}(x,Q^2). \tag{43}$$

In the following Sects. 3.2.1-3.2.2 we will provide expressions for the various contributions to Eq. (41) up to $\mathcal{O}(\alpha_s^2)$, with more explicit formulae collected in Appendix A.

For the rest of this section we shall assume that the generic structure function $F(x,Q^2)$ refers to the structure function $F_2(x,Q^2)$ in electromagnetic deep-inelastic scattering. The specific differences for the cases of both $F_L(x,Q^2)$ and weak-mediated DIS structure functions will be discussed at the end of Sec. 3.2.2.

3.2.1 Order α_s

At order α_s the matching condition for parton distributions Eq. (30) is the trivial relation $f_q^{(n_l)}(x,m^2) = f_q^{(n_l+1)}(x,m^2)$. This means that at this order all light quark and the gluon PDFs should be matched by assuming them to be continuous at $Q=m$, while the (non-intrinsic) heavy quark PDFs should be simply taken to vanish at $Q=m$. The matching condition at a generic scale Q^2, used to determine the coefficient functions B_i of Eq. (6) in terms of the original massive–scheme ones $C_i^{(n_l)}$ starts at order α_s, Eq. (34). However, Eqs. (36, 37) show that the correction is nonzero only for the gluon PDF. Since the gluon coefficient function starts at $\mathcal{O}(\alpha_s)$, it follows that the coefficient functions B_i start differing from the $C_i^{(n_l)}$ only at $\mathcal{O}(\alpha_s^2)$:

$$B_i\left(z,\frac{Q^2}{m^2},\alpha_s^{(n_l+1)}(Q^2)\right) = C_i^{(n_l)}\left(z,\frac{Q^2}{m^2},\alpha_s^{(n_l+1)}(Q^2)\right) + \mathcal{O}(\alpha_s^2). \tag{44}$$

At this order all "light" coefficient functions are the same in the massless and massive scheme:

$$C_{i,l}^{(n_l)}\left(x,\frac{Q^2}{m^2},\alpha_s(Q^2)\right) = C_{i,l}^{(n_l+1)}\left(x,\alpha_s(Q^2)\right) + \mathcal{O}\left(\alpha_s^2\right)\ , \tag{45}$$

which immediately implies that the FONLL expression of $F_l(x,Q^2)$ trivially reduces to the massless scheme one:

$$F_l^{\rm FONLL}(x,Q^2) = F_l^{(d)}(x,Q^2) + F_l^{(n_l)}(x,Q^2) = F_l^{(n_l+1)}(x,Q^2) + \mathcal{O}(\alpha_s^2). \tag{46}$$

where we have

$$F_l^{(d)}(x,Q^2) = x\sum_{i=h,\bar{h}}\int_x^1 C_{i,l}^{(n_l+1)}\left(\frac{x}{y},\alpha_s(Q^2)\right) f_i^{(n_l+1)}(y,Q^2), \tag{47}$$

$$F_l^{(n_l)}(x,Q^2) = x\sum_{i\neq h,\bar{h}}\int_x^1 C_{i,l}^{n_l+1}\left(\frac{x}{y},\alpha_s(Q^2)\right) f_i^{(n_l+1)}(y,Q^2). \tag{48}$$

[6] Note that up to $\mathcal{O}(\alpha_s^2)$ the coefficient functions are the sum of contributions which are quadratic in the quark electric charge; however at order $\mathcal{O}(\alpha_s^3)$, interference terms proportional to the product of different electric charges do arise (see Ref. [28]).

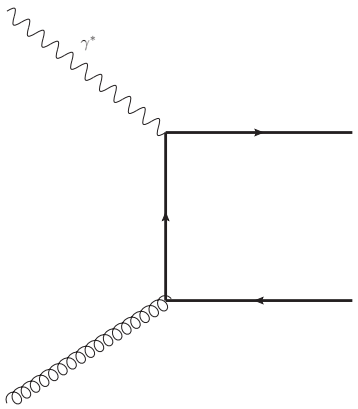

Figure 1: The $\mathcal{O}(\alpha_s)$ diagram for heavy quark production.

The "heavy" coefficient functions $C_{i,h}$, for i corresponding to any light quark are also trivially the same at order $\mathcal{O}(\alpha_s)$ in the massless and massive scheme, since they both vanish at that order, but the gluon one is different. We have

$$C_{g,\,h}^{(n_l)}\left(z,\frac{Q^2}{m^2},\alpha_s(Q^2)\right)=a_s(Q^2)2e_h^2C_g^{(n_l),1}\left(z,\frac{Q^2}{m^2}\right)+\mathcal{O}\left(\alpha_s^2\right), \tag{49}$$

where

$$\begin{aligned}C_g^{(n_l),1}\left(z,\frac{Q^2}{m^2}\right) &= \theta\left(W^2-4m^2\right)\times T_R[(z^2+(1-z)^2+4\epsilon z(1-3z)-8\epsilon^2z^2)\log\frac{1+v}{1-v}\\ &\quad +(8z(1-z)-1-4\epsilon z(1-z))v\,],\end{aligned} \tag{50}$$

with

$$\epsilon\equiv m^2/Q^2,\quad v\equiv\sqrt{1-4m^2/W^2}. \tag{51}$$

The factor of 2 associated with the squared charges in Eq. (49) accounts for the contribution of both the quark and the antiquark. This Feynman diagram for this contribution is shown in Fig. 1.

The massless limit Eqs. (10-11) of $C_{g,\,h}^{(n_l)}$ Eqs. (49-50) is

$$B_{g,\,h}^{(0),\,1}\left(z,\frac{Q^2}{m^2}\right)=2e_h^2C_g^{(n_l,0),1}\left(z,\frac{Q^2}{m^2}\right), \tag{52}$$

where, according to Eq. (10) the index 1 denotes the first order in α_s, and

$$C_g^{(n_l,0),1}\left(z,\frac{Q^2}{m^2}\right)=T_R\left[(z^2+(1-z)^2)\log\frac{Q^2(1-z)}{m^2z}+(8z(1-z)-1)\right], \tag{53}$$

which in the limit $Q^2=m^2$ reproduces the massless scheme coefficient function:

$$C_{g,h}^{(n_l+1)}\left(z,\alpha_s(Q^2)\right)=a_s2e_h^2c_g^{(n_l,0),1}\left(z,1\right)\ . \tag{54}$$

The FONLL expression for the "heavy" component is given by

$$F_h^{\rm FONLL}(x,Q^2) = F_h^{(n_l)}(x,Q^2) + F_h^{(d)}(x,Q^2). \tag{55}$$

The two contributions on the right-hand side of Eq. (55) are respectively the massive-scheme heavy-quark structure function, given by

$$F_h^{(n_l)}(x,Q^2) = x\int_x^1 \frac{dy}{y} C_{g,h}^{(n_l)}\left(\frac{x}{y},\frac{Q^2}{m^2},\alpha_s(Q^2)\right) f_g^{(n_l+1)}(y,Q^2), \tag{56}$$

with $C_{g,h}^{(n_l)}\left(\frac{x}{y},\frac{Q^2}{m^2},\alpha_s\right)$ given by Eqs. (49,50); and the "difference" contribution

$$\begin{aligned} F_h^{(d)}(x,Q^2) &= x\int_x^1 \frac{dy}{y}\left[C_{q,h}^{(n_l+1)}\left(\frac{x}{y},\alpha_s(Q^2)\right)\left[f_h^{(n_l+1)}(y,Q^2)+f_{\bar h}^{(n_l+1)}(y,Q^2)\right]+\right. \\ &\left.\left(C_{g,h}^{(n_l+1)}\left(\frac{x}{y},\alpha_s(Q^2)\right) - B_{g,h}^{(0)}\left(\frac{x}{y},\frac{Q^2}{m^2},\alpha_s(Q^2)\right)\right) f_g^{(n_l+1)}(y,Q^2)\right], \end{aligned} \tag{57}$$

where $C_{g,h}^{(n_l+1)}$ and $B_{g,h}^{(0)}$ are given by Eqs. (54),(52), respectively, and $C_{q,h}^{(n_l+1)}$ is the $\mathcal{O}(\alpha_s)$ quark coefficient function for production of a (massless) quark of charge e_h.

It is easy to see explicitly that, in the region where L is not large, the "difference" term is of order $\mathcal{O}(\alpha_s^2)$, so that to $\mathcal{O}(\alpha_s)$ the FONLL expression coincides with the massive–scheme one. Indeed, Eq. (31) implies that the heavy quark distribution is $\mathcal{O}(\alpha_s)$. Use of the leading–order QCD evolution equations immediately leads to

$$f_h(y,Q^2) = f_{\bar h}(y,Q^2) = \frac{\alpha_s(Q^2)}{2\pi} L\int\frac{dz}{z} T_f(z^2+(1-z)^2) g\left(\frac{x}{y},Q^2\right) + \mathcal{O}(\alpha_s^2). \tag{58}$$

Noting that $C_{q,h}\left(x,\alpha_s(Q^2)\right) = \delta(1-x)+\mathcal{O}(\alpha_s)$ it immediately follows that the two terms in Eq. (57) cancel up to terms of order $\mathcal{O}(\alpha_s^2)$.

3.2.2 Order α_s^2

We will now work out the FONLL expressions for structure functions at $\mathcal{O}(\alpha_s^2)$. We expand structure functions and coefficient functions in powers of $a_s^{(n_l+1)}(Q^2)$, Eq. (24), as follows:

$$C_i = \sum_{p=0}^{P}\left(\frac{\alpha_s^{(n_l+1)}(Q^2)}{2\pi}\right)^p C_i^p; \quad F^{\rm FONLL} = \sum_{p=0}^{P}\left(\frac{\alpha_s^{(n_l+1)}(Q^2)}{2\pi}\right)^p F^{{\rm FONLL},\,p}, \tag{59}$$

and similarly for other quantities. In order to deal with manageable expressions we will collect in Appendix A the expressions for the $\mathcal{O}(\alpha_s^2)$ coefficients C_i^2, $F^{{\rm FONLL},\,2}$, and so on, while the contributions up to $\mathcal{O}(\alpha_s)$ were given explicitly in Sec. 3.2.1.

At the NNLO order, both "light" and "heavy" coefficient functions differ in the massive and massless scheme. As far as "light" coefficient functions are concerned, the gluon one is the same

$$C_{g,l}^{(n_l),\,2}\left(x,\frac{Q^2}{m^2}\right) = C_{g,l}^{(n_l+1),\,2}(x), \tag{60}$$

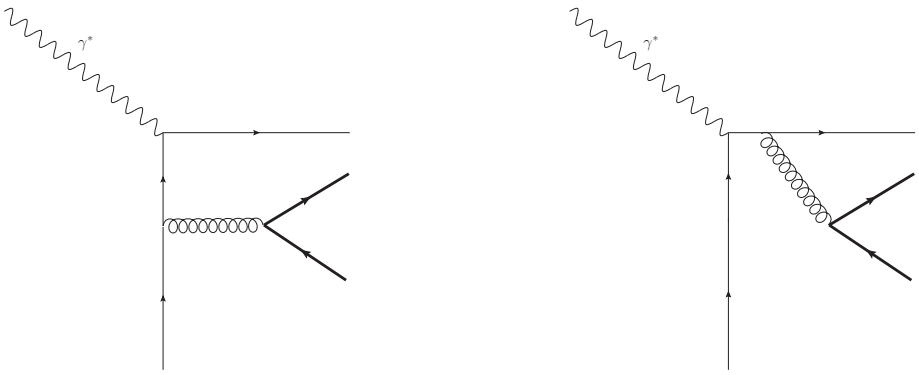

Figure 2: The $\mathcal{O}(\alpha_s^2)$ diagrams for heavy quark production which contribute to the "light" coefficient function F_l Eq. (41).

but the quark one $C_{i\neq g,\,l}^{(n_l),\,2}$ is different, because of the contribution coming from the emission of a gluon which in turns radiates a h–$\bar{h}$ pair, shown in Fig. 2.

Further contributions may arise when re–expressing the strong coupling and parton distribution in terms of their massless–scheme counterparts for quarks we find that the $\mathcal{O}(\alpha_s^2)$ contribution $B_{i,\,l}^2$ for $i \neq g$ (Eq. (9)) is given in terms of the coefficients (Eq. (59)) of the expansion of the massive–scheme coefficient function by

$$B_{i,\,l}^2\left(z, \frac{Q^2}{m^2}\right) = C_{i,\,l}^{(n_l),\,2}\left(z, \frac{Q^2}{m^2}\right) - \left[e_i^2 K_{qq}(z, L) + \frac{2T_R}{3} L C_i^{(n_l),\,1}(z)\right], \tag{61}$$

where $C_{i,\,l}^{(n_l),\,2}$ is the coefficient function for the i–th light quark or antiquark, $K_{qq}(z, L)$ is given in Eq. (40) and $C_i^{(n_l),\,1}$ is the standard [27] (massless) NLO contribution to the coefficient function for the i–th quark or antiquark. The term proportional to $C_i^{(n_l),\,1}$ arises when expressing $\alpha_s^{(n_l)}$ in terms of $\alpha_s^{(n_l+1)}$ (using Eq. (27)) in the $\mathcal{O}(\alpha_s)$ correction to $C_i^{(n_l)}(z)$. The massless limit of $B_{i,\,l}^2$ Eq. (61), for $i \neq g$ is given by

$$B_{i,\,l}^{(0),\,2}\left(z, \frac{Q^2}{m^2}\right) = C_{i,\,l}^{(n_l,0),\,2}\left(z, \frac{Q^2}{m^2}\right) - \left[e_i^2 K_{qq}(z, L) + \frac{2T_R}{3} L C_i^{(n_l),\,1}(z)\right], \tag{62}$$

where $C_{i,\,l}^{(n_l,0),\,2}$ denotes the massless limit of the coefficient function in the massive scheme.

In the gluon sector, even though the coefficient function $C_{g,\,l}^{(n_l),\,2}$ coincides with its massless counterpart, according to Eq. (60), both the expression in terms of their massless–scheme counterparts of the strong coupling Eq. (27) and of the gluon distribution Eq. (36) contribute to the determination of B_g^2 (Eq. (9)), as discussed in Sec. 3.1.2. The former contribution is of course the same as in Eq. (61), and the latter turns out to cancel it exactly, so that in the end we get

$$B_{g,\,l}^2\left(z, \frac{Q^2}{m^2}\right) = C_{g,\,l}^{(n_l),\,2}(z), \tag{63}$$

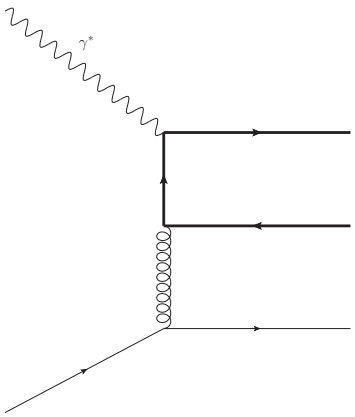

Figure 3: The light-quark initiated $\mathcal{O}(\alpha_s^2)$ diagram for heavy quark production which contributes to the "heavy" coefficient function F_h Eq. (41).

namely, the coefficient function is the same as in the massless scheme after all.

Turning now to "heavy" coefficient functions, both the quark and gluon ones, $C_{i,h}^{(n_l),2}$, with $i = q$, g are nontrivial in the massive scheme, because heavy quarks contribute both to quark–initiated (Fig. 3) and gluon–initiated processes (Fig. 4). When re-expressing in terms of the massless-scheme strong coupling and PDFs, we now find

$$B_{i,h}^2\left(z,\frac{Q^2}{m^2}\right) = C_{i,h}^{(n_l),2}\left(z,\frac{Q^2}{m^2}\right). \tag{64}$$

Indeed, for an incoming light quark the "heavy" contribution only starts at $\mathcal{O}(\alpha_s^2)$, so up to $\mathcal{O}(\alpha_s^2)$ it is unaffected by changes in the coupling and PDFs, while for an incoming gluon the argument leading to Eq. (63) also applies, and leads to the same conclusion.

Collecting this information, we can construct the FONLL expression for the various contributions to the structure function. For the "light" component $F_l(x,Q^2)$, we find that the $\mathcal{O}(\alpha_s^2)$ contribution to the FONLL expression is given by

$$F_l^{\rm FONLL,\,2}(x,Q^2) = F_l^{(d),\,2}(x,Q^2) + F_l^{(n_l),\,2}(x,Q^2), \tag{65}$$

Here the contribution to the massive-scheme structure function is

$$F_l^{(n_l),\,2}(x,Q^2) = x\sum_{i\neq h,\bar{h}}\int_x^1\frac{dy}{y}B_{i,l}^2\left(\frac{x}{y},\frac{Q^2}{m^2}\right)f_i^{(n_l+1)}(y,Q^2), \tag{66}$$

where the sum runs over light quark flavours and antiflavours and $B_{i,l}^2$ and $f_i^{(n_l+1)}$ are respectively the massive coefficient function Eq. (61) and PDF for the i–th light flavour.

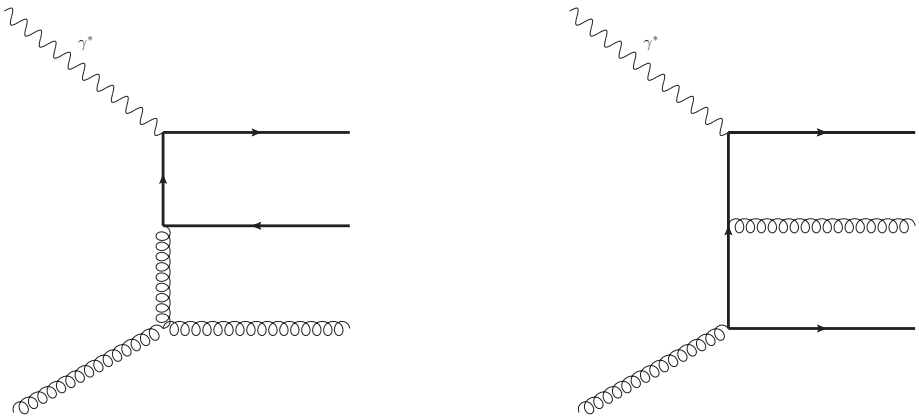

Figure 4: The gluon initiated $\mathcal{O}(\alpha_s^2)$ real diagrams for heavy quark production which contribute to the "heavy" coefficient function F_h Eq. (41).

The $\mathcal{O}(\alpha^2)$ term of the "difference" contribution is then given by

$$\begin{aligned} F_l^{d,\,2}(x,Q^2) &= x\sum_{i\neq h,\bar{h},g}\int_x^1 \frac{dy}{y}\left[C_{i,\,l}^{(n_l+1),\,2}\left(\frac{x}{y}\right) - B_{i,\,l}^{(0),\,2}\left(\frac{x}{y},\frac{Q^2}{m^2}\right)\right] f_i^{(n_l+1)}(y,Q^2) \\ &\quad + x\sum_{i=h,\bar{h}}\int \frac{dy}{y} C_{i,\,l}^{(n_l+1),\,2}\left(\frac{x}{y}\right) f_i^{(n_l+1)}(y,Q^2)\ , \end{aligned} \tag{67}$$

where $B_{i,\,h}^{(0),\,2}$ are given by Eqs. (62, 63), and the NNLO massless light quark and gluon coefficient functions $C_{i,\,h}^{(n_l+1),\,2}$, first computed in Refs. [29, 30] are respectively given in Eqs. (B.2-B.4) and Eq. (B.6) of Ref. [31].[7]

Now that the structure function is computed to $\mathcal{O}(\alpha_s^2)$, when L is not large, the difference contribution F^d must start at the order α_s^3. The second term in Eq. (67) manifestly starts at this order, since it is proportional to the product of the heavy flavour parton density, which starts at order α_s, and the coefficient function for an incoming heavy quark to produce a light quark that couples to the photon, which is of order α_s^2. In order for the first term in Eq. (67) not to be of $\mathcal{O}(\alpha_s^2)$, the difference of coefficients in the square bracket must vanish identically. Notice therefore that in actual fact the coefficient $B_{i,\,l}^{(0),\,2}\left(\frac{x}{y},\frac{Q^2}{m^2}\right)$ does not depend on Q^2/m^2. In order to verify this cancellation, we rewrite the first term on the r.h.s of Eq. (62) as

$$C_{i,l}^{(n_l,0),2}\left(z,\frac{Q^2}{m^2}\right) = \bar{C}_{i,l}^{(n_l),2}(z) + e_i^2 C^{\mathrm{NS},2}\left(z,\frac{Q^2}{m^2}\right)\ , \tag{68}$$

where $\bar{C}_{i,l}^{(n_l),2}(z)$ stands for the $\overline{\mathrm{MS}}$ coefficient function of flavour i with n_l light flavours, and

$$C^{\mathrm{NS},2}\left(z,\frac{Q^2}{m^2}\right) \equiv \frac{1}{4}\left[L_q^{\mathrm{NS},(2)}\left(z,\frac{m^2}{Q^2}\right) + L_q^{\mathrm{NS,S+V},(2)}\left(z,\frac{m^2}{Q^2}\right)\right], \tag{69}$$

[7] Note that in Ref. [31] coefficient functions are given as a series in powers of $\frac{\alpha_s}{4\pi}$.

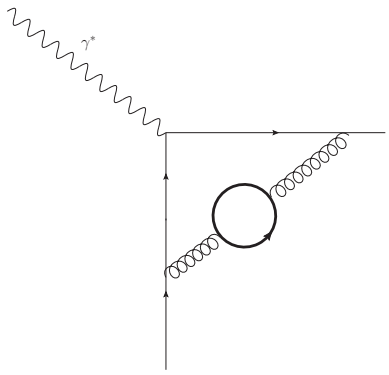

Figure 5: The light-quark initiated $\mathcal{O}(\alpha_s^2)$ diagram in which heavy quarks contribute to the gluon self-energy.

where $L_q^{\rm NS}$ is given in equations (D.8) and (D.10) of Ref. [32] and the factor of $1/4$ accounts for the fact that $\alpha_s/(4\pi)$ rather than $\alpha_s/(2\pi)$ is used in that reference. In other words, Eq. (68) splits the coefficient functions into terms not involving heavy flavours at all, and terms involving a heavy flavour,[8] like the diagrams shown in Figs. 2,5.

Since the $C_{i,l}^{(n_l+1),2}$ coefficients are also $\overline{\rm MS}$ coefficients (and since they depend linearly upon n_l), we have

$$C_{i,l}^{(n_l+1),2}(z) - \bar{C}_{i,l}^{(n_l),2}(z) = \frac{\partial}{\partial n_l} C_{i,l}^{(n_l+1),2}(z), \tag{70}$$

so that, in order for the first term of Eq. (67) to be of order α_s^3 we must have

$$\frac{\partial}{\partial n_l} C_{i,l}^{(n_l+1),2}(z) - e_i^2 C^{\rm NS,2}(z, m^2/Q^2) + \left[e_i^2 K_{qq}(z, L) + \frac{2T_R}{3} L C_i^{(n_l),\,1}(z) \right] = 0. \tag{71}$$

Using Eqs. (40), (D.8) and (D.10) of Ref. [32], and Eq. (4) of Ref. [29] for the coefficient of n_l in $C_{i,l}^{(n_l+1),2}$, we can easily verify Eq. (71).[9]

The structure of the $\mathcal{O}(\alpha_s^2)$ contribution to the FONLL expression for the "heavy" component of F is similar to that of its $\mathcal{O}(\alpha_s)$ counterpart Eq. (55), namely

$$F_h^{\rm FONLL,\,2}(x, Q^2) = F_h^{(d),\,2}(x, Q^2) + F_h^{(n_l),\,2}(x, Q^2), \tag{72}$$

except that now both light quarks and gluons contribute to the massive–scheme term:

$$F_h^{(n_l),\,2}(x, Q^2) = x \int_x^1 \frac{dy}{y} \sum_{i \neq h, \bar{h}} B_{i,h}^{(n_l),\,2}\left(\frac{x}{y}, \frac{Q^2}{m^2}\right) f_i^{(n_l+1)}(y, Q^2), \tag{73}$$

[8] By "terms not involving heavy flavours" we also mean here terms where the heavy flavour contribution totally decouples in the decoupling scheme, which is typically the case of heavy flavour loop corrections to on–shell gluon propagators.

[9] We remark here that the first moments of $C_{i,l}^{(n_l+1),2}$, $\bar{C}_{i,l}^{(n_l),2}$, $C^{\rm NS,2}(z, m^2/Q^2)$, $K_{qq}(z, L)$ and $C_i^{(n_l),\,1}$ all vanish individually. This fact, which can be explicitly verified, is a consequence of the Adler sum rule.

with the sum running over all light quark and antiquarks and gluons, and $B_{g,h}^{(n_l),\,2}$ given by Eq. (64). The real diagrams corresponding to the gluon initiated contributions to Eq. (73) are shown in Fig. 4, while the corresponding light-quark initiated contribution is shown in Fig. 3.

The difference contribution is now given by

$$F_h^{(d),\,2}(x,Q^2) = x\sum_{i=h,\bar{h}}\int_x^1 \frac{dy}{y} C_{i,h}^{(n_l+1),2}\left(\frac{x}{y}\right) f_i^{(n_l+1)}(y,Q^2) + \sum_{i\neq h,\bar{h},g}\int_x^1 \frac{dy}{y}\left[C_{i,h}^{(n_l+1),2}\left(\frac{x}{y}\right) - B_{i,\,h}^{(0),\,2}\left(\frac{x}{y},\frac{Q^2}{m^2}\right)\right] f_i^{(n_l+1)}(y,Q^2). \quad (74)$$

Here $C_{i,h}^{(n_l+1),2}$ are the massless-scheme $\mathcal{O}(\alpha_s^2)$ contributions to the standard coefficient functions for production of a quark of electric charge e_h, from Refs. [29–31] and already used in Eq. (67), with the heavy quark treated as another massless flavour, while $B_{i,\,h}^{(0),\,2}$ are the massless limits of the massive coefficient functions Eq. (64), given in Eqs. (D4,D6) of Ref. [32] for gluons and quarks respectively.

As mentioned in the beginning of Sec. 3.2, all results so far apply to the structure function $F_2(x,Q^2)$. However, they also hold for the longitudinal structure function $F_L(x,Q^2)$, whose coefficients are given in the references cited above along with those for F_2. The only difference is that, because the structure function $F_L(x,Q^2)$ starts at $\mathcal{O}(\alpha_s)$ also in the light quark sector, for this structure function one finds the simplified expression

$$B_{i,\,l;\,L}^2\left(z,\frac{Q^2}{m^2}\right) = C_{i,\,l;\,L}^{(n_l),\,2}\left(z,\frac{Q^2}{m^2}\right) - \frac{2T_R}{3} L C_i^{(n_l),\,1}(z) \quad (75)$$

instead of the more complicated relation Eq. (61).

While we have provided up to now explicit results for electromagnetic DIS structure functions, it is straightforward to generalize the above discussion to the case of weak-mediated neutral current DIS: indeed, the only modifications consists of the replacement of the electromagnetic charges by the corresponding weak charges.

The generalization to charged–current (CC) DIS is slightly more complicated. Firstly, full $\mathcal{O}(\alpha_s^2)$ CC coefficient coefficient functions are not available: only their asymptotic $Q^2 \gg m^2$ limits [33] and their threshold behaviour [34] are currently known, so that the FONLL can only be implemented to this order. For CC scattering initiated by a heavy quark, like strangeness production though $W-$boson exchange, the FONLL formulae of Sec. 3.2.1 straightforwardly generalize, taking into account only the different charges and kinematics. On the other hand, for CC scattering with a light quark in the initial state, such as charm production in neutrino scattering (commonly known as "dimuon production") the heavy quark PDF does not enter, so the FONLL results reduces to the massive calculation (with scheme ambiguities only entering at $\mathcal{O}(\alpha_s^2)$).

3.3 Structure functions: schemes and perturbative ordering

Various possibilities for the definition of perturbative ordering are possible and have been advocated, especially in the context of parton fits including DIS data. This is due to the fact that LO parton distributions can be used for the computation of any hard process

at the first nonvanishing oder: it is then natural to adopt a "relative" definition of perturbative ordering, where LO is the lowest nontrivial order at which the process starts occurring. This is to be contrasted with an "absolute" definition of perturbative ordering, such that LO refers to $\mathcal{O}(\alpha_s^0)$ (parton model), NLO to $\mathcal{O}(\alpha_s)$, and so forth. The issue is nontrivial because in a global parton fit one may want to combine data for the total structure function F, which starts at $\mathcal{O}(\alpha_s^0)$, and those for the heavy structure function F_h, which starts at $\mathcal{O}(\alpha_s)$.

One option is then to simply adopt an absolute perturbative ordering, whereby at NLO all quantities are computed at $\mathcal{O}(\alpha_s^2)$. This choice has been adopted for instance in the CTEQ parton fits [1]. We will refer to it as scheme A henceforth. However, as discussed in Sec. 2.2 we can also consistently use different accuracies in the computation of different contributions. At NLO we can then compute the total structure function at $O(\alpha)$, but use the $\mathcal{O}(\alpha_s^2)$ results of Sec. 3.2.2 for the determination of F_h (both with NLO PDFs). In such case, it is not necessary to compute any of the massless-scheme coefficient functions $C_i^{(n_l+1)}$ beyond NLO (i.e. beyond $\mathcal{O}(\alpha_s)$) because this does not improve the accuracy of the NLO calculation in the massless sector, but all massive coefficient functions B_i^2 and their massless limits $B_i^{(0),\,2}$ should be computed to $\mathcal{O}(\alpha_s^2)$ in order to have this accuracy in the massive sector. In order to ensure consistency of the subtraction it is sufficient to include only logarithmic terms in $B_i^{(0),\,2}$, because the corresponding non-logarithmic terms are not included in the massless coefficient functions $C_i^{(n_l+1)}$. We will refer to this as scheme B.

This scheme B is reminiscent of the method proposed in Refs . [8–10], and used e.g. in MSTW PDF fits [14]: there too, the $\mathcal{O}(\alpha_s^2)$ expression of the massive cross section is used in conjunction with NLO parton densities and coefficient functions, although within a totally different approach.

We can then also pursue a full $\mathcal{O}(\alpha_s^2)$ computation, by simply performing the absolute-orderd computation of scheme A to one extra order, with NNLO PDFs. We will refer to this as scheme C. However, we cannot pursue scheme B to one extra order because $\mathcal{O}(\alpha_s^3)$ massive coefficient functions are not known yet, though their large Q^2 limit was recently determined in Ref. [35]. In NNLO MSTW fits [14] they have been modelled based on their known large– and small x behaviour.

In summary, we will consider three options for perturbative ordering, whose consistency will be checked explicitly in the following Sec. 3.4, and whose phenomenological implications will be discussed in Sec. 4, namely:

- Scheme A: the $\mathcal{O}(\alpha_s)$ FONLL expressions of Sec. 3.2.1 with NLO parton densities.
- Scheme B: the $\mathcal{O}(\alpha_s^2)$ FONLL expressions of Sec. 3.2.2, but using NLO parton densities and $\mathcal{O}(\alpha_s)$ massless coefficient functions, and retaining the $\mathcal{O}(\alpha_s^2)$ contributions to the massive coefficient functions. In this case, the massive expression exceeds in accuracy the massless one when L is not large. Thus, according to section 2.2, in the massless limit expression of Eq. (15), the non-logaritmic $\mathcal{O}(\alpha_s^2)$ term in $F^{(n_l,0)}$ should not be included.

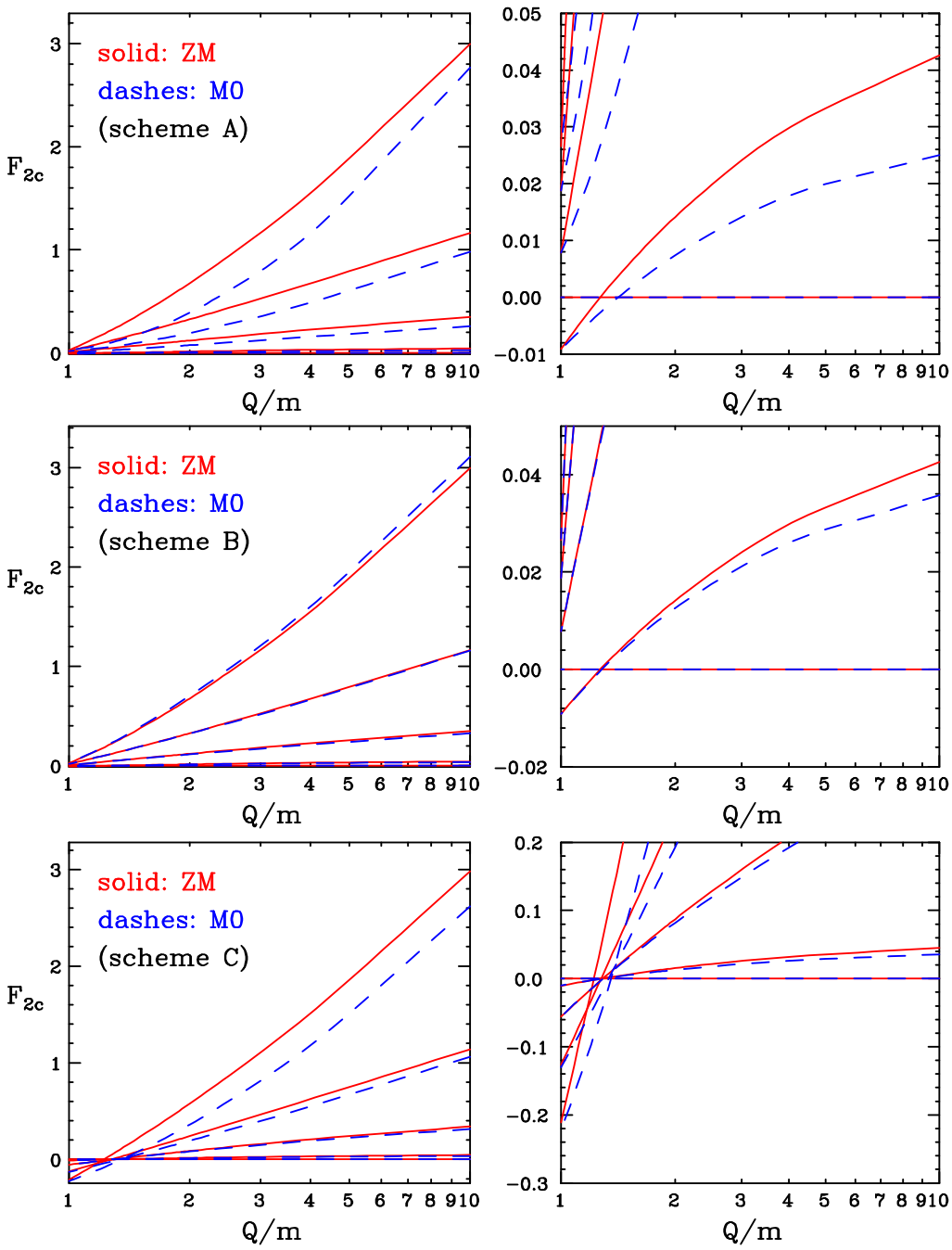

Figure 6: The $F_{2\,c}$ structure function computed in the massless scheme Eq. 1 (ZM) and in the massless limit of the massive scheme Eq. (12) (M0), in the three perturbative ordering schemes A-C of Sec. 3.3. The structure function is plotted as a function of Q/m, for $x = 10^{-\frac{5}{4}(j-1)}$, with integer $1 \leq j \leq 5$ (from top to bottom at large Q/m). The plots on the right show a magnification of the threshold region.

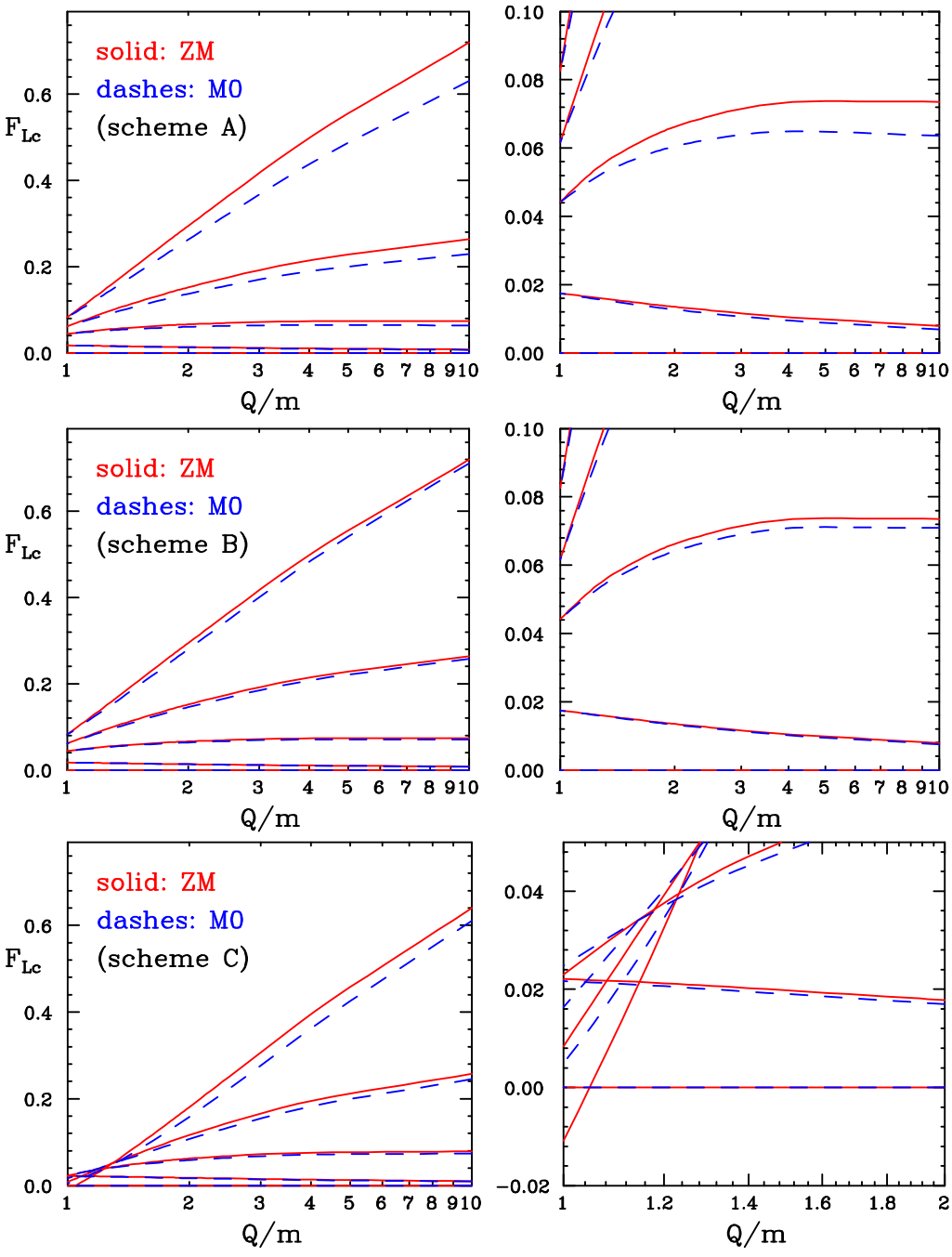

Figure 7: Same as Fig. 6, but for the structure function $F_{L\,c}(x, Q^2)$.

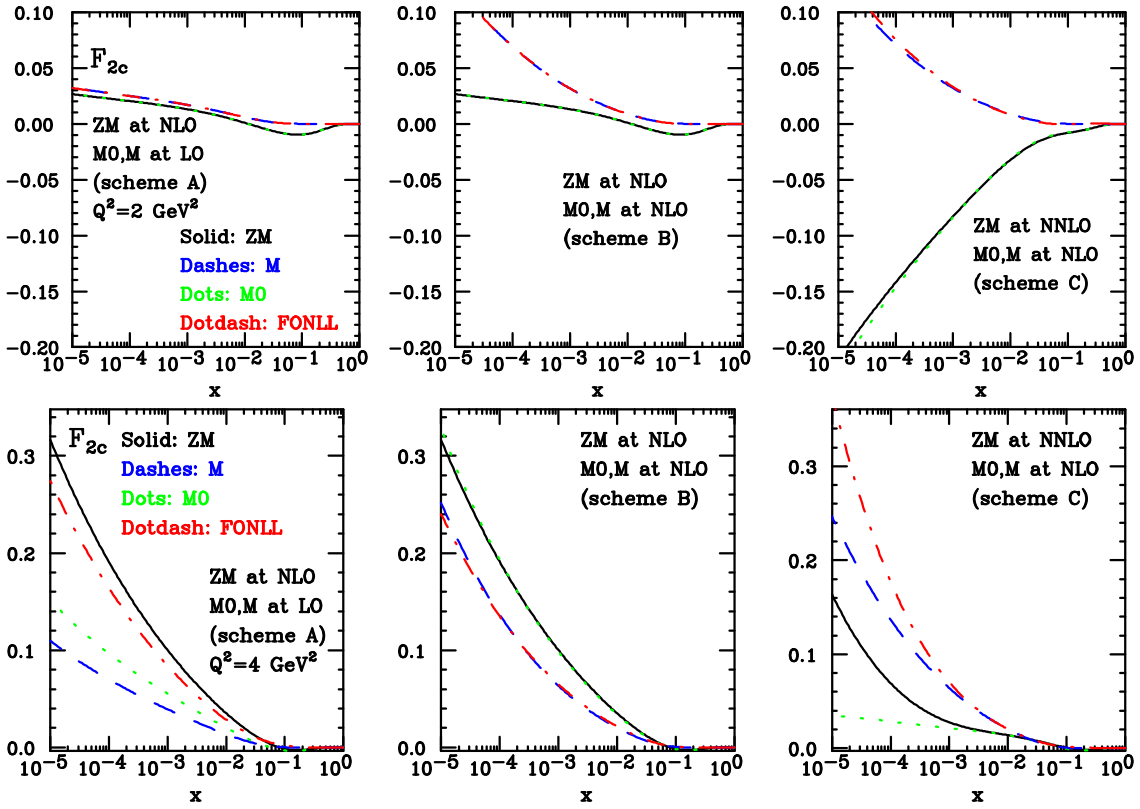

Figure 8: The $F_{2\,c}$ structure function computed in the massive scheme Eq. 2 (M), massless scheme Eq. 1 (ZM), massless limit of the massive scheme Eq. (12) (M0) and FONLL scheme Eq. (14). The schemes adopted in the three columns correspond to the different combinations of perturbative orders discussed in Sec. 3.3. Results at the scales $Q^2 = m_c^2 = 2$ GeV^2 and $Q^2 = 4$ GeV^2 are given in the two rows.

- Scheme C: the $\mathcal{O}(\alpha_s^2)$ FONLL expressions of Sec. 3.2.2 with NNLO parton densities.

We address now the question of the relation of the FONLL scheme with other approaches. As already said, our B scheme is reminiscent of the TR scheme, although it is certainly not identical to it. The complexity of the TR implementation has prevented us from obtaining a clearer view of the differences.

Our A scheme is easily shown to be equivalent to the SACOT variant of the ACOT scheme. If a χ-scaling prescription is also applied (with the same definition used by the ACOT group), the A scheme becomes equivalent to the SACOT-χ one. There is no analog of our B scheme within ACOT. A full discussion of ACOT at NNLO as not yet appeared in the literature. We believe, however, that our C scheme should be equivalent to SACOT at the NNLO level, or at least we do not see any reason why it should differ from it. A benchmarking of the FONLL, ACOT and TR prescription, which in particular confirms that FONLL and SACOT-χ agree to NLO, has been recently performed in Ref. [36]

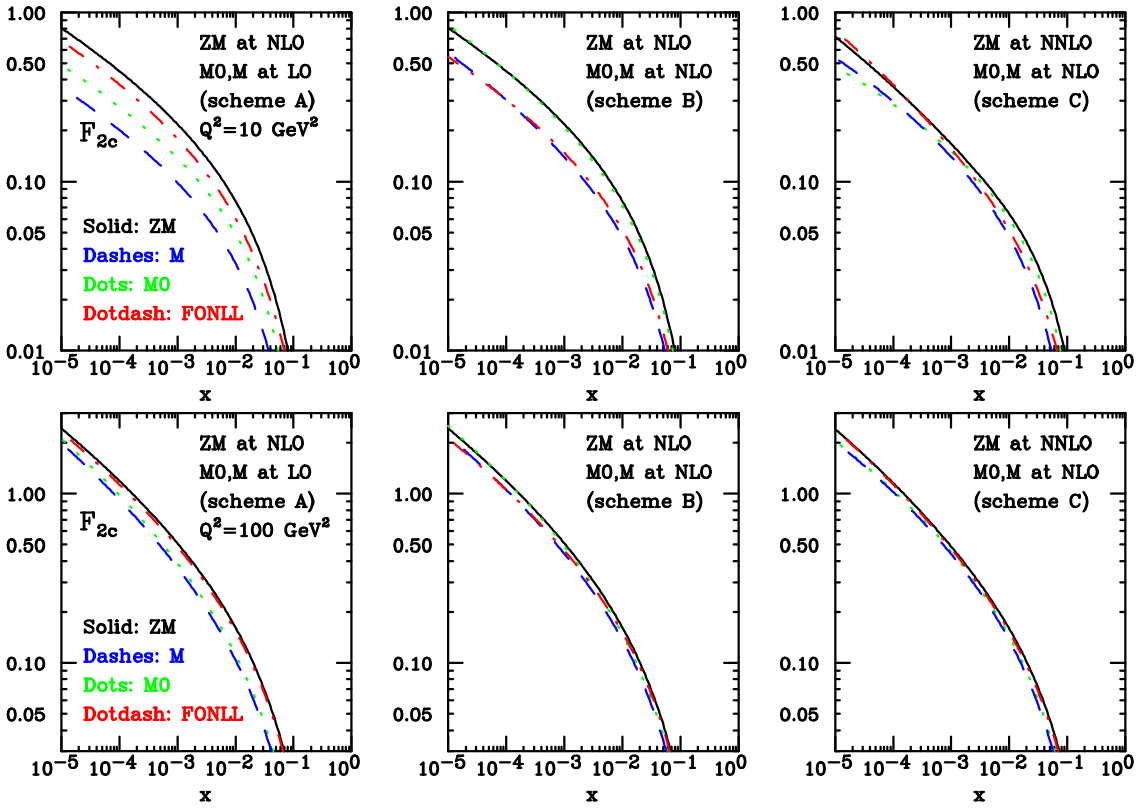

Figure 9: Same as Fig. 8, but at the higher scales $Q^2 = 10$ and $Q^2 = 100$ GeV^2. Note that a log scale is now adopted in the y–axis.

Recently, the BMSN prescription which we briefly discussed in Sect. 2.1 after Eq. (16), has also been used for PDF determination in Ref. [19]. On top of the differences already mentioned there between the FONLL and BMSN approaches, in Ref. [19] the resummation of powers of L Eq. (5) which we discussed at length in Sect. 2.1 is not performed [20]: this may be adequate in PDF determinations which do not use data at large Q^2, but it requires a subsequent transformation to a scheme where such a resummation is included for the sake of phenomenology at large Q^2, as indeed done in Ref. [19].

3.4 Consistency of the FONLL procedure

The consistency of the FONLL method is guaranteed by the subtraction of the overlapping terms from the massless result, as implemented in Eq. (14). Ideally, one should be able to verify that, in the $m \to 0$ limit and with light flavour PDFs fixed at the scale Q^2, the massless scheme (ZM, henceforth) result Eq. (1) and the zero–mass limit of the massive (M0, henceforth) result Eq. (12) should coincide up to higher orders in α_s. This is in practice quite difficult in general [37]; however, several features that must hold in the relation between the ZM and M0 result near threshold are rather easier to verify: in this section we will perform some of these checks, thereby verifying the consistency of

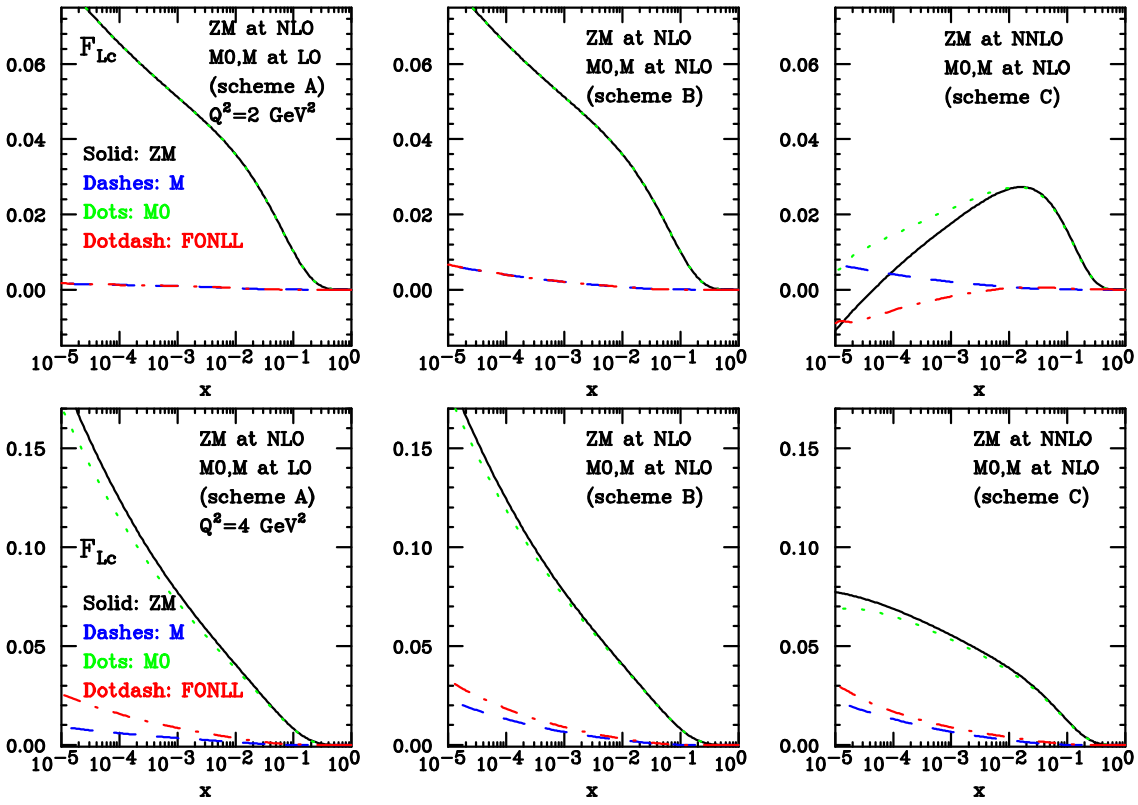

Figure 10: Same as Fig. 8, but for the structure function $F_{L\,c}$.

the FONLL procedure. The discussion which follows applies to a generic deep-inelastic "heavy"structure function $F_h(x,Q^2)$ Eq. (41): we will show explicit results for both the structure functions $F_{2\,h}(x,Q^2)$ and $F_{L\,h}(x,Q^2)$.

Recall how the perturbative expansion and the logarithms of Q^2/m^2 are organized in the ZM and M0 result. The "heavy" structure function $F_h(x,Q^2)$ in the massless scheme Eqs. (1,41) is given by

$$F_h^{(n_l+1)}(x,Q^2) = x\int_x^1 \frac{dy}{y}\left[C_{h,h}^{(n_l+1)}\left(\frac{x}{y},\alpha_s(Q^2)\right)\left(h(y,Q^2)+\bar{h}(y,Q^2)\right)\right. \tag{76}$$
$$\left. +C_{q,h}^{(n_l+1)}\left(\frac{x}{y},\alpha_s(Q^2)\right)\sum_q\left(q(y,Q^2)+\bar{q}(y,Q^2)\right)+C_{g,h}^{(n_l+1)}\left(\frac{x}{y},\alpha_s(Q^2)\right)g(y,Q^2)\right],$$

where the choice of scheme for α_s and PDFs is immaterial.

For the sake of a comparison between the ZM and M0 results, the heavy quark PDFs $h,\bar{h}$ can be viewed as a function of $L=\log\left(Q^2/m^2\right)$, with the light parton densities $g(y,Q^2)$ and $q(y,Q^2)$ treated as constants. At NLO we get

$$h(y,Q^2)\equiv\sum_{i=1,\infty}h_i^{(0)}(y)\alpha_s^i L^i+\sum_{i=2,\infty}h_i^{(1)}(y)\alpha_s^i L^{i-1}. \tag{77}$$

Decomposing the coefficient functions as

$$C_{h,h}^{(n_l+1)} = C_{h,h}^{(n_l+1),0} + \alpha_s C_{h,h}^{(n_l+1),1}, \qquad C_{g,h}^{(n_l+1)} = \alpha_s C_{g,h}^{(n_l+1),1}, \qquad C_{q,h}^{(n_l+1)} = 0\,. \quad (78)$$

the ZM structure function is, up to NLO

$$F_h^{(n_l+1)}(x,Q^2) = x\int_x^1 \frac{dy}{y}\left[C_{h,h}^{(n_l+1),0}\left(\frac{x}{y}\right)\left(\alpha_s(Q^2)h_1^{(0)}(y) + \alpha_s^2(Q^2)h_2^{(1)}(y)\right)L \right. \quad (79)$$
$$\left. + C_{h,h}^{(n_l+1),1}\left(\frac{x}{y}\right)\left(h_1^{(0)}(y)\alpha_s^2(Q^2) + h_2^{(1)}(y)\alpha_s^3(Q^2)\right)L + C_{g,h}^{(n_l+1),1}\left(\frac{x}{y}\right)\alpha_s(Q^2)g(y,Q^2) + \mathcal{O}\left(L^2\right)\right].$$

On the other hand, the ZM result can be written as a power series in L by expanding the coefficient function as

$$C^{(n_l,0)}\left(x, L, \alpha_s(Q^2)\right) \equiv \sum_{i=1}^{N}\sum_{j=0}^{i} C^{(n_l,0),i,j}(x)\alpha_s(Q^2)^i L^j. \quad (80)$$

In scheme A of Sec. 3.3, which corresponds to using NLO with fixed–order results consistently included up to $\mathcal{O}(\alpha_s)$ result, one gets

$$F_h^{(n_l,0)}(x,Q^2) = x\int_x^1 \frac{dy}{y}\left[C_{g,h}^{(n_l,0),1,0}\left(\frac{x}{y}\right)\alpha_s(Q^2)g(y,Q^2)\right.$$
$$\left. + C_{g,h}^{(n_l,0),1,1}\left(\frac{x}{y}\right)\alpha_s(Q^2)g(y,Q^2)L\right]. \quad (81)$$

Therefore, because of Eq. (54) the ZM result Eq. (79) and the M0 result Eq. (81) must coincide when $L = 0$, while their slope in L near $L = 0$ should differ by terms of order α_s^2, which are present in the ZM Eq. (79) but not in the M0 result Eq. (81). This is borne out by the plots Fig. 6 for $F_{2\,c}(x,Q^2)$ and Fig. 7 for $F_{L\,c}(x,Q^2)$, in which the structure function is plotted as a function of Q/m for several values of x (with $m = m_c = \sqrt{2}$ GeV). We have also checked that the difference in slope is indeed of order α_s^2, by repeating the plot with different values of α_s^2.

In scheme B, which corresponds to NLO but with $\mathcal{O}(\alpha_s^2)$ contributions included in massive coefficient functions, the M0 result becomes

$$F_h^{(n_l,0)}(x,Q^2) = x\int_x^1 \frac{dy}{y}\left[C_{g,h}^{(n_l,0),1,0}\left(\frac{x}{y}\right)\alpha_s(Q^2)g(y,Q^2)\right.$$
$$+ C_{g,h}^{(n_l,0),1,1}\left(\frac{x}{y}\right)\alpha_s(Q^2)Lg(y,Q^2) + C_{g,h}^{(n_l,0),2,1}\left(\frac{x}{y}\right)\alpha_s(Q^2)^2 Lg(y,Q^2)$$
$$\left. + C_{q,h}^{(n_l,0),2,1}\left(\frac{x}{y}\right)\alpha_s(Q^2)^2 L\sum_q\left(q(y,Q^2) + \bar{q}(y,Q^2)\right) + \mathcal{O}\left(L^2\right)\right], \quad (82)$$

which now also receives a contribution from the light–quark initiated terms of Fig. 2, which start at $\mathcal{O}\left(\alpha_s^2\right)$. Note that, as already mentioned in Sec. 3.3, in scheme B non-logarithmic $\mathcal{O}\left(\alpha_s^2\right)$ are not included in the M0 result, because they must match the ZM result, which in this scheme is determined at NLO, so that beyond $\mathcal{O}\left(\alpha_s\right)$ it only contains logarithmically enhanced terms. Comparing the M0 result Eq. (82) to the ZM one of Eq. (79) one sees

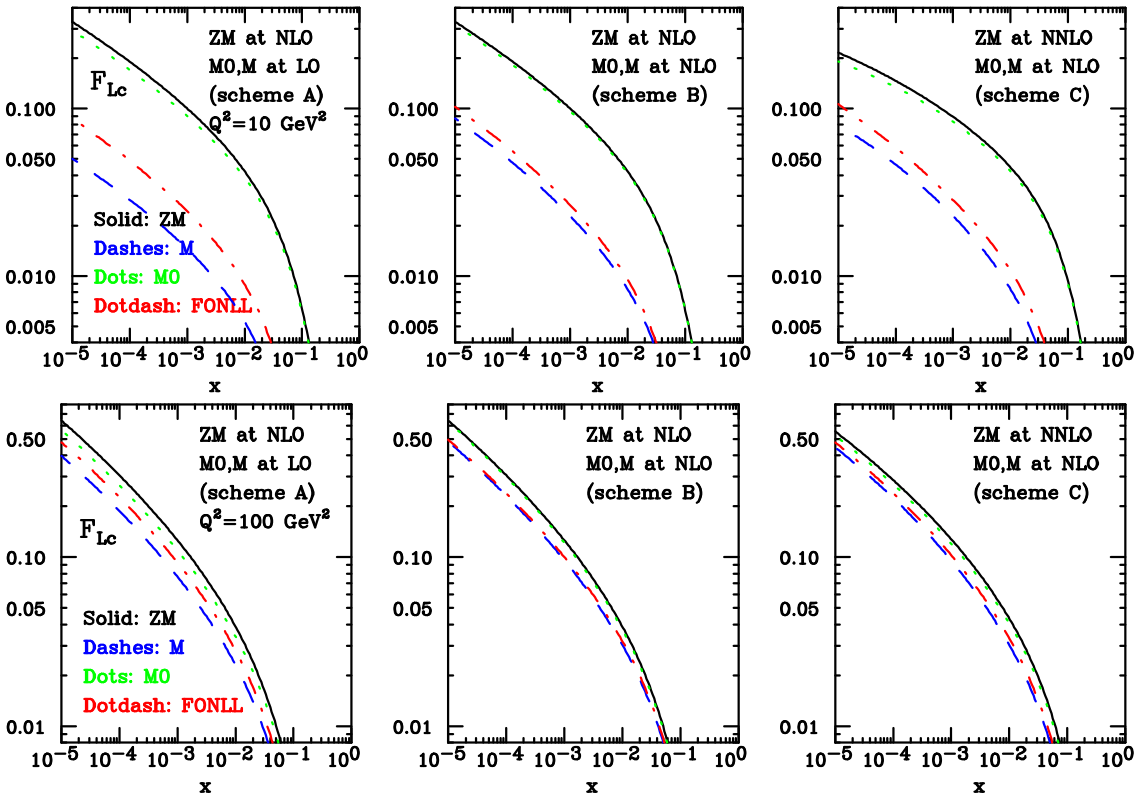

Figure 11: Same as Fig. 9, but for the structure function $F_{L\,c}$.

that in scheme B not only the value at threshold but also the slope should agree, up to a small correction $\mathcal{O}\left(\alpha_s^3\right)$ due to contribution proportional to $h_2^{(1)}$ in Eq. (79). This is borne out by the plots in Figs. 6–7.

The same reasoning can be pursued to NNLO. In this case, we only have results in scheme C, in which fixed–order results are included up to $\mathcal{O}(\alpha_s^2)$. In this case the ZM and M0 results differ at threshold both in value and slope through terms of order α_s^3 arising both from the PDF and the coefficient function. This mismatch is apparent in Figs. 6–7, and turns out to be quantitatively different in $F_{2\,c}$ and in $F_{L,\,c}$. Indeed, for $F_{2\,c}$ (Fig. 6) the difference in slope is very visible, but the difference in value at $L = 0$ is very small and difficult to appreciate. On the other hand for $F_{L\,c}$ (Fig. 7), higher order corrections are larger and the differences also in values at threshold are more visible.

4 Phenomenological impact of the FONLL method

We will now examine the phenomenological impact of the FONLL method on structure functions. We will consider the case, both for F_2 and F_L, of the total structure function, as well as the "heavy" contribution F_h to structure functions in the particular case of charm, namely $F_{2\,c}$ and $F_{L\,c}$. The purpose of our study is to assess the impact of heavy quark terms at various perturbative orders, to compare and validate different prescriptions

for the treatment of subleading terms close to threshold, and finally to provide a general assessment of the impact of heavy quarks on structure functions. A study of the impact of heavy quark terms on a determination of PDFs should be part of a global PDF fit and it is thus beyond the scope of our work.

In order to ease comparison with other studies, we will use the PDFs of the standard reference Les Houches [38] set at the scale $Q_0^2 = 2$ GeV^2, evolved using the `QCDNUM` [39] package, and tabulated in Refs. [38, 40] both in the massive and massless scheme (with, in the latter case, PDFs matched according to the results given in Sec. 3.1.1). Massive $\mathcal{O}(\alpha_s^2)$ contributions to coefficient functions have been determined using the numerical implementation of the results of Ref. [21], and their massless limit using the numerical implementation of the results of Ref. [32]. All the analytic expressions which we have used and the computer codes used to implement them are illustrated in the Appendix A. As in Ref. [38], we take the charm mass at $m^2 = 2$ GeV^2 and $\alpha_s(m_c^2) = 0.35$, which corresponds to values in the ballpark $\alpha_s(M_z^2) \sim 0.120$ at NLO and $\alpha_s(M_z) \sim 0.110$ at NNLO according to the scheme used (see Refs. [38, 40] for the exact values). We will furthermore neglect the b threshold, by letting $m_b \to \infty$.

4.1 Comparison between FONLL, massive and massless results

At first, we compare structure functions in the massive scheme Eq. (2) (M, henceforth), in the massless scheme Eq. (1) (ZM, henceforth), in the massless limit of the massive scheme Eq. (12) (M0, henceforth), and using the FONLL prescription Eq. (14). We begin by showing in the first three plots of Fig. 8 the structure function $F_{2\,c}$, computed using the three different combinations of perturbative orders discussed in Sec. 3.3 and referred to as schemes A–C, at the charm mass scale $Q^2 = m_c^2 = 2$ GeV^2. We see that in all cases the ZM and M0 results either coincide, or else are very close, as we have already seen in Sec. 3.4. It follows that the "difference" contribution Eq. (15) is vanishingly small, and thus FONLL result coincides with the massive calculation.

However, the same quantities at $Q^2 = 4$ GeV^2 (also displayed in Fig. 8) show remarkable differences. In the scheme A, the ZM and M0 results differ considerably, so FONLL no longer simply reduces to the massive result, and it is in fact rather closer to the ZM result. This is not the case in scheme B, in which the ZM and M0 results again nearly coincide. The case of scheme C is similar to that of scheme B for $x > 10^{-3}$, but for smaller values of x the ZM and M0 result again differ considerably. In Fig. 9 we see that this pattern persists at higher energies, although with a reduced impact of mass effects. This means that inclusion of the $\mathcal{O}(\alpha_s^2)$ contribution to the massive terms in scheme B significantly reduces the impact of the unreliable $\mathcal{O}(\alpha_s^2)$ terms in the difference contribution which are present in scheme A, and whose effect persists even at larger scales. However, in scheme C further $\mathcal{O}(\alpha_s^3)$ terms are introduced, which may become large at small x due to large small x logs [41].

From the plot on the first column of Fig. 9, we also see that the difference between the M0 and M curves (i.e. the impact of mass effects) in the first order heavy flavour coefficient is quite large even at a scale of 10 GeV^2. This difference seems to be reduced in the third column, which suggests a cancellation of mass effects between the first and second order in α_s. This cancellation should be considered accidental, and it cannot be taken as evidence that mass effects are negligible at this scale.

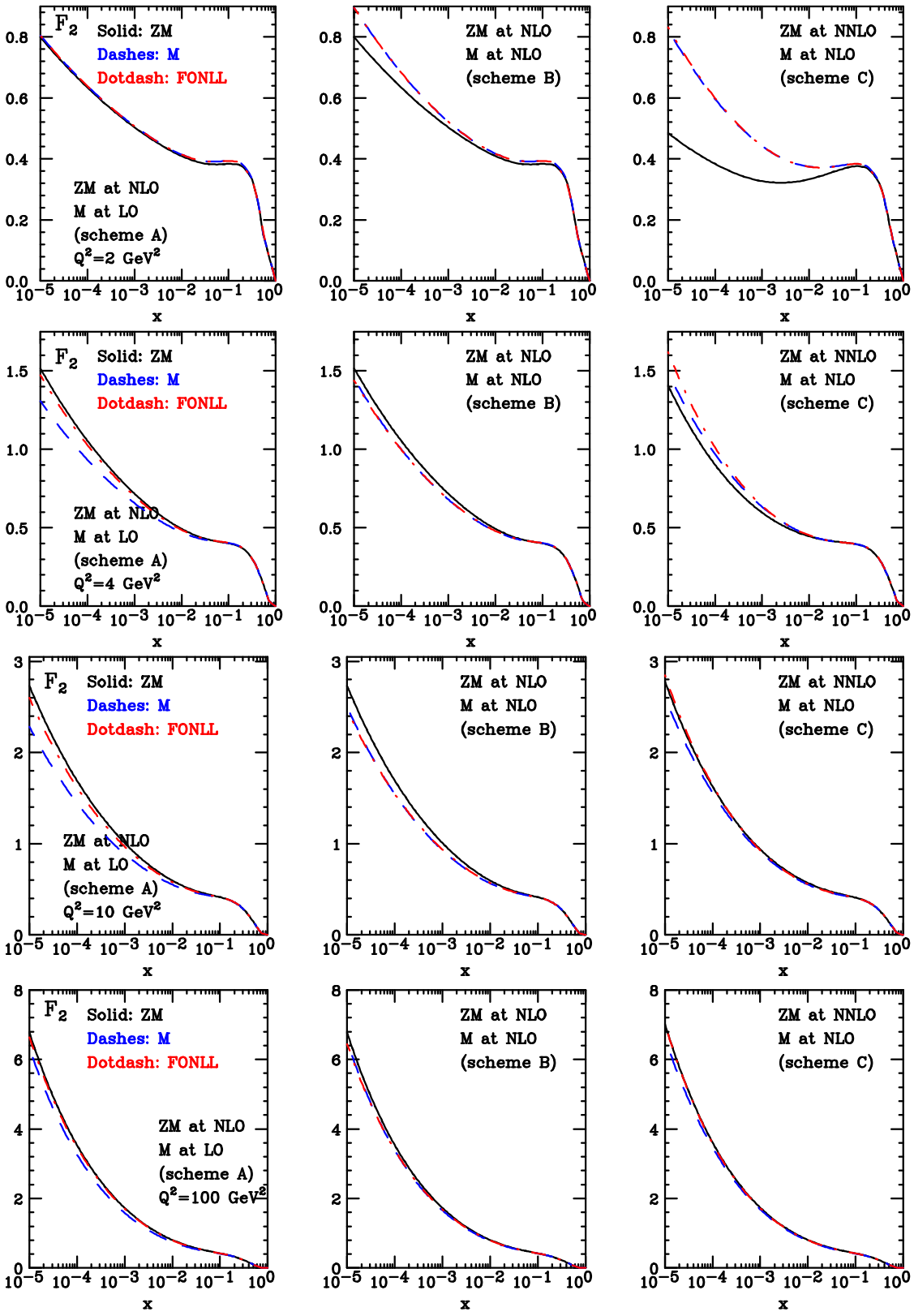

Figure 12: Same as Figs. 8–9 but for the total structure function F_2.

We now turn to the structure function $F_{L\,c}$. Also in this case, right at threshold (Fig. 10) the ZM and M0 results compensate exactly in the A and B schemes, though now in scheme C they start to deviate at $x \lesssim 10^{-2}$, and only coincide for larger x values. As the scale is raised to $Q^2 = 4$ GeV^2, the ZM and M0 results start to differ, though by a much smaller amount than in the case of $F_{2\,c}$. In this case, however, the ZM and M0 results at and close to threshold are much larger in magnitude than the M result. This means that for $F_{L,c}$ the massless approximation is completely inadequate close to threshold. This is clarly seen in Fig. 10, where the massless result at threshold in all cases A-C is totally different from the massive one, to which instead FONLL essentially reduces in cases A-B, because of the complete cancellation between the M and M0 terms. In case C, however, the M and M0 terms do not cancel completely at threshold (recall Fig. 7, especially the lower right plot) and thus, because of the the large relative size of these (subleading and unphysical) terms in comparison to the massive result, the FONLL result ends up having also an unphysical behaviour at threshold. This means that in this case it is crucial to implement a suppression of these subleading terms as discussed in Sect. 2.3, and that this suppression must be very strong at threshold (as it is using the threshold factor Eq. (19)): only in such case the difference contribution Eq. (15) is removed and FONLL reproduces the M result again. Obviously, this means that the impact of the threshold prescription for F_L in scheme C is very strong. Once again, at $Q^2 = 10$ GeV^2 (Fig. 11) the M and M0 results differ considerably. Even at $Q^2 = 100$ GeV^2 mass effects are not at all negligible for $F_{L\,c}$.

In Figs. 12-13 we turn to the to the total structure functions, i.e. the sum of the light and heavy contributions Eq. (41). As discussed in Sec. 3.2, the FONLL prescription has no effect on F_l to $O(\alpha_s)$, and thus is scheme A. Its effect to $O(\alpha_s^2)$, which comes from the Feynman diagrams of Figs. 2-5 is very small: the contribution from these diagrams is small in the first place, and its contribution to the FONLL prescription is further suppressed by the cancellation Eqs. (70-71). Therefore, the dominant effect of the FONLL prescription is on F_h, and thus diluted in the total structure functions. Nevertheless, the main qualitative features remain the same. Namely, in scheme A a significant difference between the massive and FONLL results arises just above the threshold, and persists up to scales as large as 10–20 GeV^2, with the FONLL result rather closer to the massless one for F_2 and to the massive one for F_L. This difference is driven by subleading (unreliable) threshold contributions, and thus sensitive to the threshold treatment discussed in Sec. 2.3, to be studied phenomenologically in Sec. 4.2. Its effects are greatly reduced in schemes B-C (but with some small x instability in scheme C) and in general for the structure function F_L.

4.2 Comparison and impact of threshold prescriptions

As explained in Sec. 2.3 the purpose of threshold prescriptions is to modify subleading contributions to the FONLL expression which are certainly not accurate but may be non-negligible close to threshold. As such, from a theoretical point of view all threshold prescriptions (including the choice of not implementing any threshold prescription) are

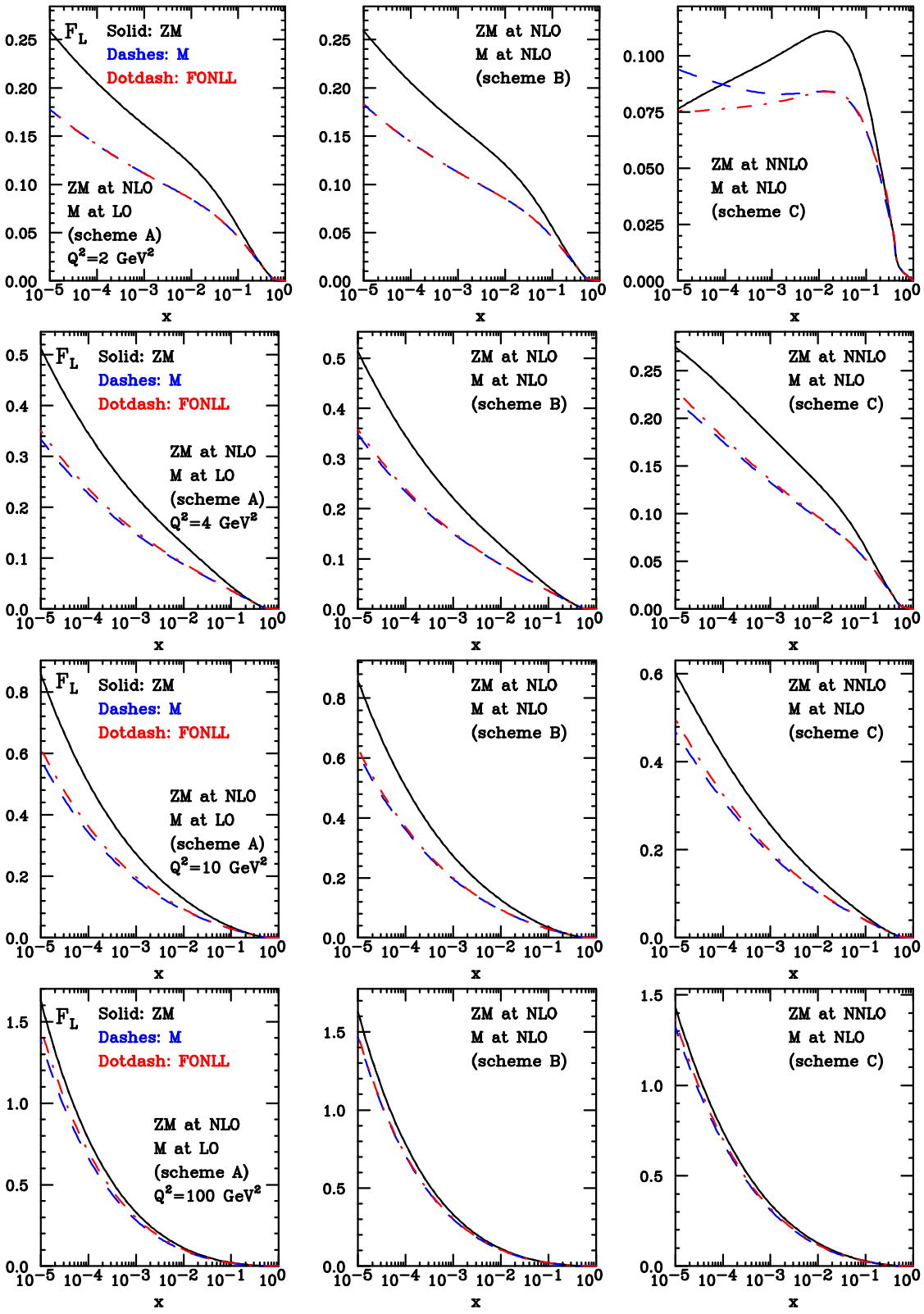

Figure 13: Same as Figs. 10–11 but for the total structure function F_L.

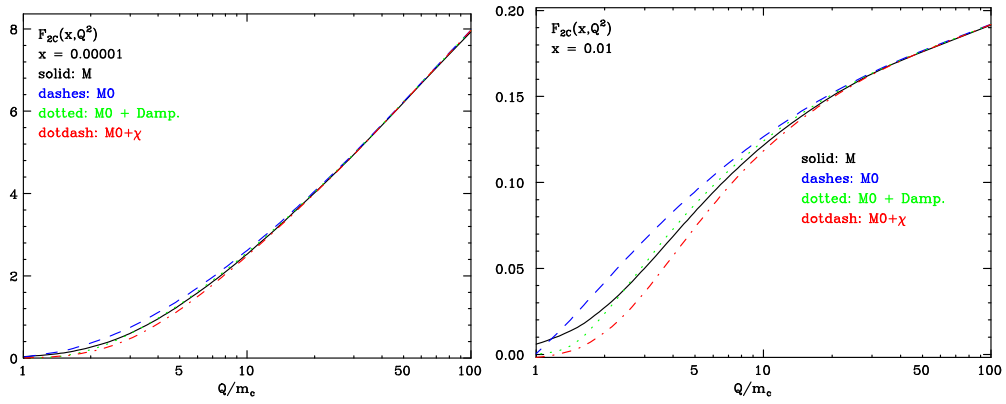

Figure 14: The $\mathcal{O}(\alpha_s)$ contribution to the charm structure function, $F_{2\,c}(x,Q^2)$ with $m_c^2 = 2$ GeV^2 plotted as a function of Q^2 at fixed x at small x. The four curves correspond to the the full massive–scheme (M) result Eq. (6), its $m \to 0$ limit (M0) Eq.(12), and the results obtained applying to the M0 a damping factor Eq. (18) or χ–scaling Eq. (20).

equally justified, and varying the threshold prescription merely provides an estimate of unknown subleading terms. However, when the higher order exact result is known we may validate the threshold prescription by comparing the subleading terms which are affected by the threshold prescription with their exact form. Here we perform such a validation; then we assess the impact of different choices for the threshold prescription on the final FONLL result.

The terms which are affected by the threshold prescription are the difference between the ZM and M0 expressions: they are nonzero because the ZM contains contributions to all orders, while the M0 is determined at fixed perturbative order. In the simplest (trivial) case in which the structure function is determined at $\mathcal{O}(\alpha_s^0)$, the massive contribution to the FONLL expression vanishes: the FONLL expression then reduces to the massless scheme one which we know to be inaccurate close to threshold. A threshold prescription applied at this order might then reduce the difference between the massless scheme expression and one in which mass effects are properly treated. In fact, in Ref. [15] the use of a massless scheme supplemented by the χ–scaling threshold prescription was advocated as a possible approximation to schemes were mass effects are fully included such as the FONLL scheme discussed here.

Of course, the first massive contribution appears at $\mathcal{O}(\alpha_s)$, so in order to assess whether indeed a threshold prescription does help we should compare the exact $\mathcal{O}(\alpha_s)$ massive (M) result, i.e. $F^{(n_l)}(x,Q^2)$ Eq. (6) to its massless (M0) approximation $F^{(n_l,0)}(x,Q^2)$, which is included in the massless (ZM) result, and to the putatively improved versions of the M0 which are obtained by supplementing it with a threshold prescription, such as the damping factor Eq. (18) or χ–scaling Eq. (20). This comparison is performed in Figs. 14-15 for the $F_{2\,c}$ structure function. We see that at very small x mass effects are small, but that for $x \gtrsim 0.01$ close to threshold the deviation between the M result and its M0 approximation becomes significant, the full result being suppressed by mass effects in comparison to its massless approximation. The threshold factor reproduces well this suppression especially at smaller x values, while χ–scaling provides a bit too much suppression and accordingly

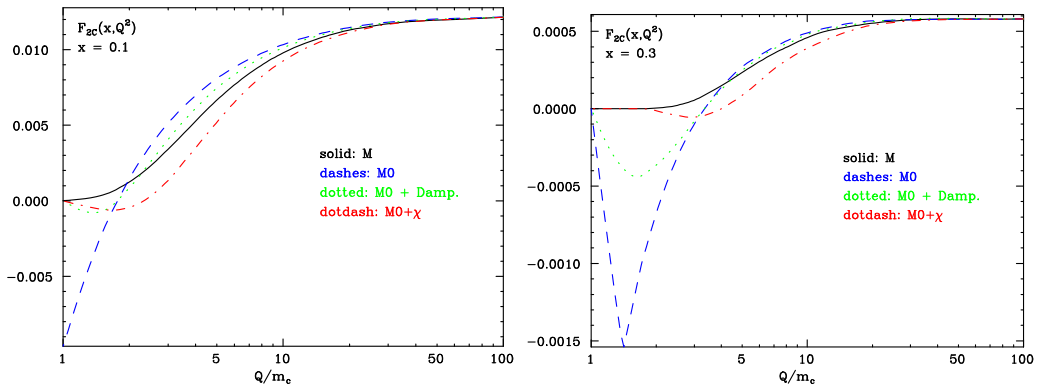

Figure 15: Same as Fig. 14 but at large x.

a somewhat worse approximation. That χ–scaling provides an excess of suppression for F_2 was already noticed in Ref. [26], where modified, improved χ variable were suggested to remedy this situation. It is interesting to observe that the slightly different χ–scaling prescription Eq. (23) (discussed in Ref. [14]) leads instead to rather less suppression, and in particular, at small x, less than the damping factor.

Our results so far, Figs. 14-15, show that indeed a threshold factor may help, but they are of academic interest as soon as we implement the FONLL prescription at lowest nontrivial order, because $\mathcal{O}(\alpha_s)$ terms are then treated exactly. We thus turn to the more practically relevant case of the $\mathcal{O}(\alpha_s^2)$ terms: these are treated approximately if we adopt the NLO FONLL method of scheme A. In Figs. 16-17 we repeat the comparison of the M, M0, and threshold–corrected M0 results, but now for the $\mathcal{O}(\alpha_s^2)$ contributions to $F_{2\,c}$. Now the difference between the exact M and approximate M0 result is significant even at very small x. It is still true that, while results with threshold prescriptions are closer to the exact one, χ–scaling provides a somewhat excessive suppression. However, now at large x the damping factor provides insufficient suppression, so the quality of the approximation of either threshold prescription is similar, though perhaps the damping factor is still slightly better on average.

If the FONLL method is treated including massive contributions up to $\mathcal{O}(\alpha_s^2)$, i.e. using schemes B or C the threshold prescription only starts affecting $\mathcal{O}(\alpha_s^3)$ terms. We can then no longer assess its accuracy, because exact $\mathcal{O}(\alpha_s^3)$ massive coefficient functions are unknown.

We can now study the impact of various threshold prescriptions on the FONLL result. This is done in Figs. 18-19, where we compare respectively the FONLL expression for the structure functions $F_{2\,c}$ and $F_{L\,c}$, determined at different perturbative orders, i.e. within schemes A-C, and either without any threshold prescription, or with either of the two threshold prescriptions that we discussed so far. The effect of the threshold treatment is most visible just above threshold at $Q^2 = 4$ GeV^2, as expected based on the discussion of Sec. 4.1 and Figs. 9-8. At this scale, in scheme A the effect of the threshold suppression procedure is visible for all values of x; in schemes B-C, where the threshold treatment only affects $\mathcal{O}(\alpha_s^3)$ terms, the effect is generally small (except, in scheme C, for very small or very large values of x). Therefore, we conclude that the ambiguity related to subleading

terms is substantially reduced if massive terms are treated to $\mathcal{O}(\alpha_s^2)$, i.e. using schemes B or C. If massive terms are treated to $\mathcal{O}(\alpha_s)$, i.e. using scheme A, our results suggests that the accuracy can be improved using a threshold suppression, and in particular using a damping factor to treat threshold effects. It is interesting to observe that, for F_2, right at threshold the difference between scheme A and scheme B appears to be non-negligible, i.e. $\mathcal{O}(\alpha_s^2)$ have a significant impact at threshold, rather larger than the typical size of the ambiguity related to threshold terms.

In the case of F_L results at threshold in scheme A show numerical instabilities due to imperfect cancellation between the ZM and M0 contributions, which as shown in Fig. 10 are much larger than the massive result. They are the consequence of the fact that the massless approximation is completely inadequate at threshold for this observable. As soon as the scale is raised above threshold this may lead to very large unphysical contributions even in the FONLL scheme unless a strong threshold suppression is adopted, such as that provided by a damping factor. This is even more the case in scheme C: due to the instability displayed in Fig. 10 results without threshold treatment, and even those obtained using χ scaling are unphysical except at very large x.

4.3 Comparison of results at different orders

Finally, in Figs. 20-21 we compare results for the structure functions F_2 and F_L determined at various perturbative orders, i.e. in the three schemes A,B,C. All results are now determined using our default option, namely, the FONLL method with the threshold treated using a damping factor: the curves are thus the same as those shown in Figs. 18-19 for the damping factor prescription. For comparison, we also show the simple massless–scheme result Eq. (1), determined at NLO ($\mathcal{O}(\alpha)$).

First, it appears that effects due to the heavy quark mass are not only large in the threshold region, but in fact still sizable at $Q^2 \sim 10$ GeV^2 for F_2, and for F_L quite large even at $Q^2 \sim 100$ GeV^2. Also, it is clear that while the B-C scheme curves are very close to each other, the curve in the A scheme differs substantially from them. This means that scheme B is an improvement over scheme A, in that it already includes most of the $\mathcal{O}(\alpha^2)$ effects which are fully included in scheme C.

Of course, because of asymptotic freedom, differences between results obtained using different perturbative schemes become smaller at large Q^2. Note however that here, for illustrative purposes, structure functions have been determined with a fixed set of PDFs. In a realistic situation, the structure function would be fixed by the data and the PDFs would be fitted.

5 Mass singularities in $F_{2\,h}$

The heavy contribution to structure functions is experimentally accessible, and indeed the experimental determination of the charm and beauty structure functions $F_{2\,c}$ and $F_{2\,b}$ has attracted considerable interest recently, in particular at HERA: specifically, the kinematic coverage of $F_{2\,c}$ data in the (x, Q^2) plane for the combined HERA-I dataset [42] is shown in Fig. 22. However, the experimental definition of heavy structure functions differs somewhat from the definition, given in Sec. 3.2, where F_h was defined as the contribution

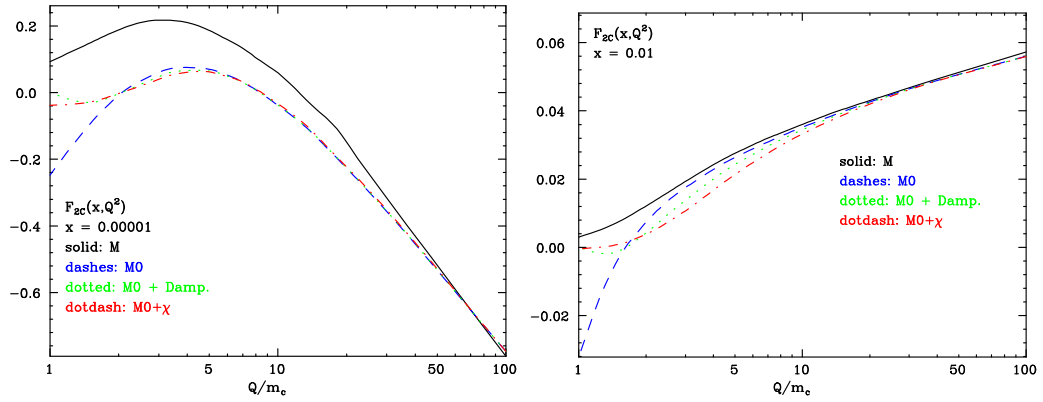

Figure 16: Same as Fig. 14 but for the $\mathcal{O}(\alpha_s^2)$ contribution to $F_{2\,c}(x, Q^2)$.

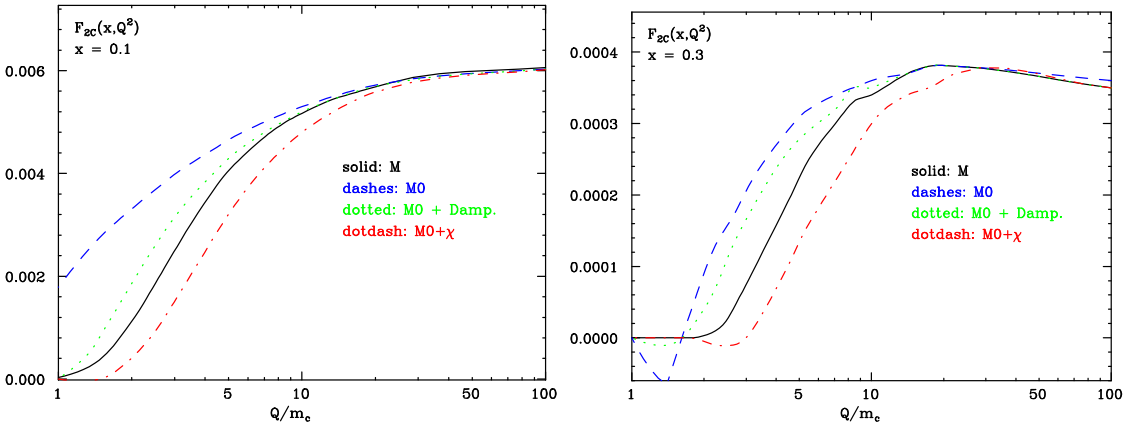

Figure 17: Same as Fig. 16 but at large x.

to the structure function F obtained when only the electric charge e_h of the heavy quark is nonzero. Rather, the experimentally measured heavy quark structure function, which we will denote by $\widetilde{F}_h$, is defined as the contribution to the structure function F from all processes in which there is a heavy quark in the final state [43–50].

The difference between $\widetilde{F}_h$ and F_h is potentially significant, because $\widetilde{F}_h$ is affected by mass singularities in the limit $m \to 0$, due to the fact that heavy–quark production contributions in which the virtual photon couples to a light quark such as shown in Fig. 2 are included in $\widetilde{F}_h$, but virtual corrections such as shown in Fig. 5 are not. In contrast, using the alternative definition F_h neither contribution is included, and both contribute to F_l, leading to a cancellation of potential mass singularities.

For finite values of the heavy quark mass these mass–singular contributions to $\widetilde{F}_h$ are of course finite, but enhanced by double logs (powers of L^2): the first diagram of Fig. 2 leads to a contribution of order $\alpha_s^2 \log^3 Q^2/m^2$ [32,37]. The three logarithmic powers have the following origin: one arises from the collinear singularity in the emission of the gluon

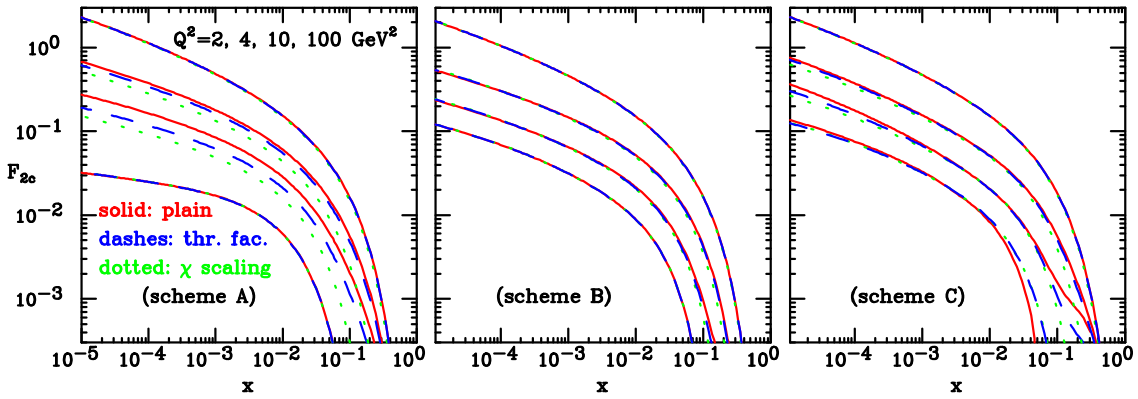

Figure 18: The FONLL expression for $F_{2\,c}$ in the three schemes for perturbative ordering A–C of Sec. 3.3, and either with no threshold suppression terms, or with the damping factor or χ scaling suppression at threshold. The structure functions are plotted as a function of x for fixed $Q^2 = 2,\ 4,\ 10,\ 100$ GeV^2 (from bottom to top).

from the light quark, one from the collinear singularity of the gluon splitting into the $h\bar{h}$ pair, and one is due to the gluon becoming soft. The latter log arises because the contribution to the coefficient function from the diagram of Fig. 2 is singular at $z = 1$: the convolution integral with the PDF up to the kinematic limit $z = Q^2/(Q^2 + m^2) < 1$ then leads to an extra log whatever the behaviour of the PDF. At higher perturbative orders $\widetilde{F}_h$ then receives double–logarithmic contributions of the form $\alpha_s^{2+k} L^{3+2k}$. These contributions could in principle be controlled experimentally by tagging both the heavy quark and antiquark and introducing a cutoff on the invariant mass of the heavy quark–antiquar pair [37].

In conventional parton fits, F_h is usually computed and compared to data, even though the data really refer to $\widetilde{F}_h$. Furthermore, even if the theoretical expression $\widetilde{F}_h$ were implemented in a parton fit, one may still wonder whether this quantity may be subject to large higher–order corrections, because of the aforementioned double logs. It is thus interesting to assess the size of the difference between $\widetilde{F}_h$ and F_h both at lowest nontrivial order and at higher orders.

5.1 Order α_s^2

We have computed the ratio

$$\Delta F_{2\,c}^{(n_l)}(x,Q^2) \equiv \frac{\widetilde{F}_{2\,c}^{(n_l)}(x,Q^2) - F_{2\,c}^{(n_l)}(x,Q^2)}{F_{2\,c}^{(n_l)}(x,Q^2)} \tag{83}$$

for the more practically relevant case of the charm structure function F_2. We use the $\mathcal{O}(\alpha_s^2)$ expressions for $\widetilde{F}_{2\,c}^{(n_l)}(x,Q^2)$ and $F_{2\,c}^{(n_l)}(x,Q^2)$ of Sec. 3.2.2: the numerator of Eq. (83) then is the contribution from the diagram of Fig. 2. Since we are mostly interested in the behaviour near threshold, the massive scheme is adopted throughout. The conventional Les Houches PDFs of Sec. 4 are used. Results are shown in Fig. 23. For comparison, we

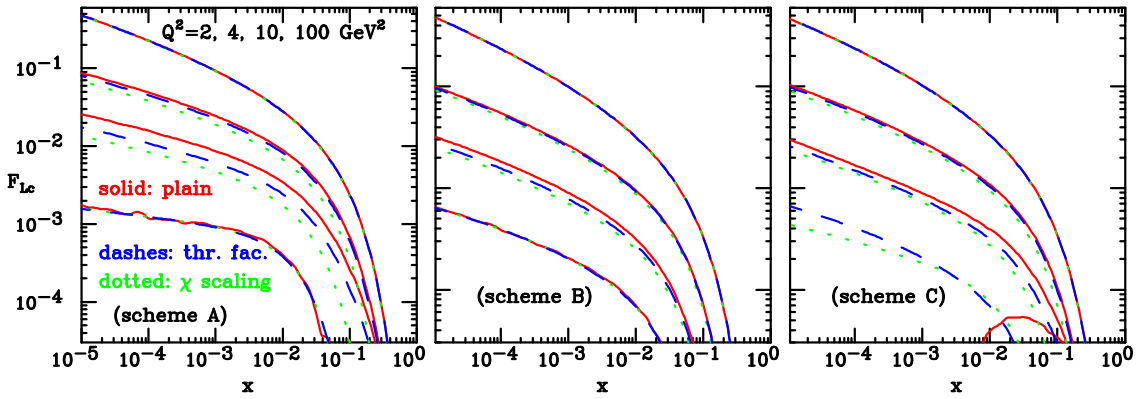

Figure 19: Same as Fig. 18 but for the structure function $F_{L\,c}$.

also show in Fig. 24 the relative size

$$R_{\rm light} \equiv \frac{F_{2\,c}^{(n_l)}\Big|_{q_i,\bar{q}_i}(x,Q^2)}{F_{2\,c}^{(n_l)}(x,Q^2)} \ , \tag{84}$$

of the contribution from the light–quark initiated diagrams $F_{2\,c}^{(n_l)}\Big|_{q_i,\bar{q}_i}$ (shown in Fig. 3) to the heavy structure function $F_{2\,c}^{(n_l)}$. It appears that the light–quark initiated contribution to $F_{2\,c}^{(n_l)}$ of Fig. 24, though moderate, can amount to as much as 10% of $F_{2\,c}$ in the HERA region and it is thus rather larger than the mass–singular contribution Fig. 23, which remains at the percent level in this region. Therefore, within this kinematics the mismatch Eq. (83) between the two definitions of the heavy quark structure function is negligible even when the measured light–quark initiated countribution (which includes both of the contributions of Figs. 23-24) is not small.

Even so, one may wonder whether these results still hold once experimental cuts are accounted for. To this purpose, we have computed

$$\Delta\sigma_{\rm vis,c} \equiv \frac{\widetilde{\sigma}_{\rm vis,c} - \sigma_{\rm vis,c}}{\sigma_{\rm vis,c}} \ , \tag{85}$$

where $\sigma_{\rm vis,c}$ is the so–called "visibile" reduced cross section (after subtraction of the contribution from F_L), i.e. the contribution to the DIS charm production cross section with experimental cuts. We have used the `HVQDIS` Monte Carlo program [51] and massive–scheme ZEUS-S PDFs [52]; hadronization and charm decay corrections have been neglected, though their inclusion would be straightforward. In order to define the visible cross section, we have assumed $p_T^c \geq 1.5$ GeV and $-1.6 \leq \eta_c \leq 2.3$, which correspond to the acceptance of the recent ZEUS muon analysis [49] when hadronization and charm decay corrections are neglected.

Our results are summarized in Table 1, where we also tabulate the percentage ratio Eq. (83) already shown in Fig. 23, but now also computed using `HVQDIS` and ZEUS-S PDFs. We have adopted an (x, Q^2) binning similar to that of the upcoming combined

HERA $F_{2\,c}$ dataset. We observe that, in qualitative agreement with the results of Fig. 23, the percentage discrepancy is always $\leq \mathcal{O}(1\%)$, reaching $\geq \mathcal{O}(2\%)$ only for the largest Q^2 bins, where statistical uncertainties are anyway much larger. Clearly, with this choice of kinematics, results are only marginally affected by experimental acceptances. We conclude that in the HERA kinematic range the discrepancy between $\widetilde{F}_h$ and F_h at $\mathcal{O}(\alpha_s^2)$ is at the level of the percent, even with experimental cuts. It is interesting to observe that at small x and not too high Q^2 this contribution grows, and it should then be properly accounted for if $F_{2\,c}$ were measured at a future higher energy electron–proton collider [53].

5.2 All–order resummation

When more gluon splitting processes are inserted in the gluon propagator in Fig. 2, before the final splitting into the $h\bar{h}$ pair, they lead to corrections enhanced by further powers of $\alpha_s \log^2 Q^2/m^2$ (i.e. double log enhanced). The effect of the complete resummation of these double logarithms was studied in detail in Ref. [54] (see also Ref. [55]), in the case of heavy flavour production associated with the production of a gluon jet at a scale Q^2. It amounts to an enhancement of the production cross section by a factor $n_g(Q^2, K^2)$, where K^2 is the virtuality of the $h\bar{h}$ pair. The way n_g is determined and its precise definition are discussed Ref. [54]; here, we can interpret it as the enhancement of the light–quark initiated heavy quark contribution of Fig. 2, i.e. the numerator of Eq. (83), whose relative size is shown in Fig. 23. We have $K^2 \geq 4m^2$, and Q^2 can be identified with the DIS Q^2 scale.

The reason why the scale Q^2 should be chosen as the scale for the evaluation of n_g, as opposed to W^2, deserves a comment, given that in the small x limit these two scales are widely different. In fact, if we assume a behaviour like $1/x^{1+\delta}$ for the light quark density in the small x limit, the contribution of the first diagram of Fig. 2 has the form

$$\int_x^{z_{max}} \frac{dz}{z} \left(\frac{\alpha_s}{4\pi}\right)^2 L_q^{\mathrm{NS},(2)}(z, Q^2/m^2) q(x/z) \approx q(x) \left(\frac{\alpha_s}{4\pi}\right)^2 \int_0^{z_{\max}} dz z^\delta L_q^{\mathrm{NS},(2)}(z, Q^2/m^2) \; . \tag{86}$$

Since $L^{\mathrm{NS},(2)}$ is a non-singlet coefficient function, its z integral is finite at the lower limit, and the result grows like $\log^3 Q^2/m^2$ (see Eq. (D.8) and subsequent comment in Ref. [32], see also Ref. [37]). This confirms the scale choice of Q^2 rather than W^2.

The function n_g is plotted in Fig. 25 as a function of K^2 for different scales Q^2: at a scale $K^2 = 4m^2 = 8$ GeV^2, we see that the enhancement is below 20% for $Q^2 \leq 100$ GeV^2, and below 90% for $Q^2 \leq 1000$ GeV^2. Hence, the effect is moderate in the HERA region, where the contribution which is thus enhanced amounts to a few percent of the structure function in the first place, as shown in Fig. 23. However, the effect becomes large as Q^2 increases and it could be a significant correction at a higher energy electron–proton collider such as the LHeC [53]. Also, in the very small x limit, single log enhanced contributions of the form $\alpha_s \log W^2/m^2$ will arise [41], and eventually prevail on the double logarithms discussed above. The effect of these small-x logarithms is unlikely to be important the HERA energy regime, but it may deserve further studies.

$x_{\min}$	$x_{\max}$	$Q^2_{\min}$ [GeV^2]	$Q^2_{\max}$ [GeV^2]	$\Delta F_{2\,c}^{\rm theo}$ (%)	$\Delta\sigma_{\rm vis,c}^{\rm theo}$ (%)
0.00002	0.00005	1.5	3.0	0.2	0.3
0.00005	0.00013	1.5	3.0	0.2	0.2
0.00013	0.00026	1.5	3.0	0.2	0.6
0.00026	0.00044	1.5	3.0	0.3	0.4
0.00005	0.00013	3.0	5.3	0.4	0.2
0.00013	0.00026	3.0	5.3	0.3	0.1
0.00026	0.00068	3.0	5.3	0.3	0.2
0.00068	0.00125	3.0	5.3	0.3	0.1
0.00010	0.00015	5.3	9.3	0.4	0.5
0.00015	0.00024	5.3	9.3	0.4	0.6
0.00024	0.00040	5.3	9.3	0.2	0.5
0.00040	0.00065	5.3	9.3	0.2	0.4
0.00065	0.00120	5.3	9.3	0.3	0.2
0.00120	0.00200	5.3	9.3	0.4	0.2
0.00014	0.00025	9.3	16.0	0.3	0.9
0.00025	0.00041	9.3	16.0	0.3	0.9
0.00041	0.00065	9.3	16.0	0.2	0.2
0.00065	0.00115	9.3	16.0	0.4	0.4
0.00115	0.00187	9.3	16.0	0.3	0.3
0.00026	0.00043	16.0	27.5	0.3	0.7
0.00043	0.00065	16.0	27.5	0.4	0.4
0.00065	0.00108	16.0	27.5	0.4	0.4
0.00108	0.00193	16.0	27.5	0.4	0.3
0.00193	0.00425	16.0	27.5	0.4	0.3
0.00425	0.00750	16.0	27.5	0.4	0.3
0.00045	0.00070	27.5	47.5	0.4	0.5
0.00070	0.00110	27.5	47.5	0.3	0.2
0.00110	0.00190	27.5	47.5	0.4	0.3
0.00190	0.00280	27.5	47.5	0.4	0.3
0.00280	0.00435	27.5	47.5	0.4	0.3
0.00435	0.00687	27.5	47.5	0.5	0.3
0.00135	0.00250	47.5	90.0	0.4	0.4
0.00250	0.00410	47.5	90.0	0.5	0.5
0.00410	0.00650	47.5	90.0	0.6	0.5
0.00650	0.01000	47.5	90.0	0.6	0.5
0.00150	0.00260	90.0	160.0	0.5	0.5
0.00260	0.00435	90.0	160.0	0.6	0.6
0.00435	0.00775	90.0	160.0	0.6	0.6
0.00775	0.02100	90.0	160.0	0.8	0.7
0.02100	0.04000	90.0	160.0	1.2	0.7
0.00375	0.00900	160.0	300.0	0.7	0.7
0.00900	0.01625	160.0	300.0	1.0	0.9
0.00975	0.01900	300.0	700.0	1.3	1.2
0.01900	0.03125	300.0	700.0	1.7	1.5
0.02250	0.03750	700.0	1500.0	2.4	2.4

Table 1: The percentage contribution of non-vanishing terms in the $e_c = 0$ limit to $F_{2\,c}$, Eq. (83), and to $\sigma_{\rm vis,c}^{\rm theo}$, Eq. (85). The grid in (x, Q^2) assumed is similar to that of the combined HERA $F_{2\,c}$ dataset, see Fig. 22.

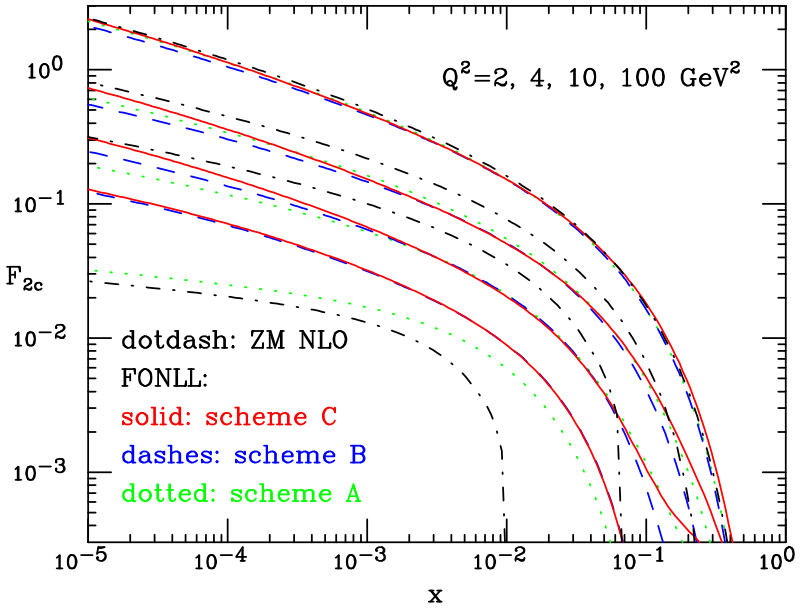

Figure 20: The FONLL expression for the structure function $F_{2\,c}$ with the threshold treated using the damping factor Eq. (18), in the three schemes for perturbative ordering A–C of Sec. 3.3. The structure functions are plotted as a function of x for fixed $Q^2 =$ 2, 4, 10, 100 GeV^2 (from top to bottom). Results in the NLO massless scheme result (same as Figs. 8-9) are also shown for comparison (dotdashed).

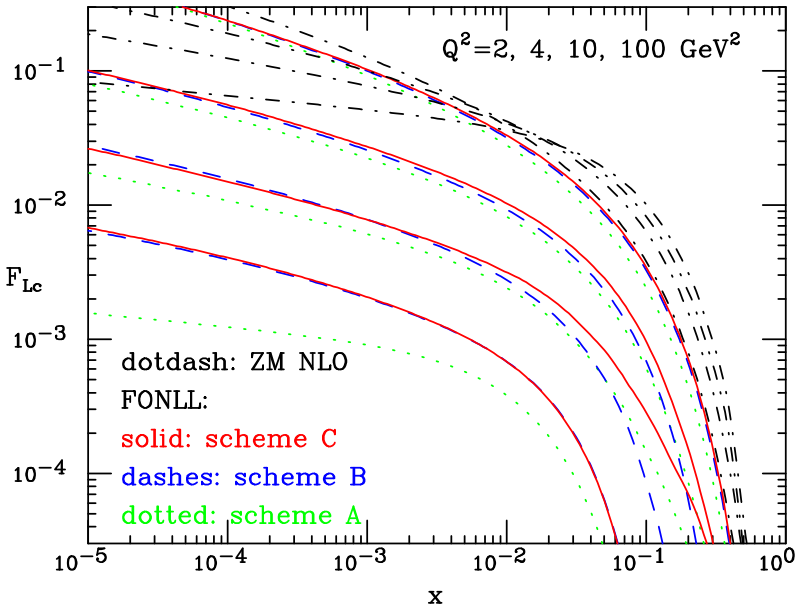

Figure 21: Same as Fig. 21, but for the structure function F_L.

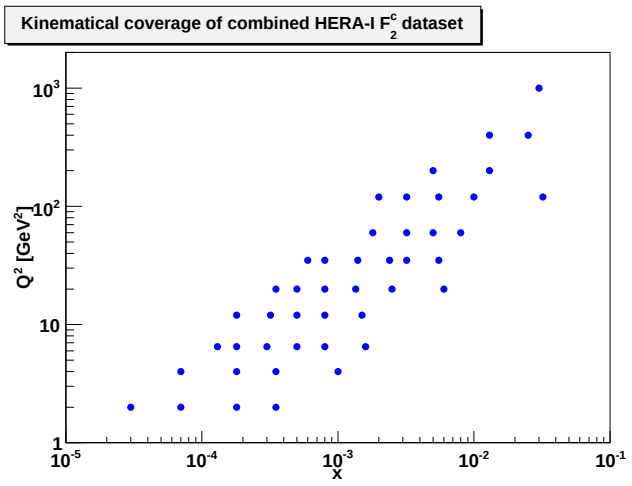

Figure 22: Kinematical coverage of $F_{2\,c}$ in the combined HERA-I [42] dataset.

6 Conclusion and outlook

We have presented a study of the theory and the phenomenology of the inclusion of heavy quark corrections in deep–inelastic structure functions, using the FONLL approach that had been previously proposed in the context of heavy quark photo— and hadroproduction. This approach is suitable for the combination of fixed order heavy quark emission terms with the all–order resummation of collinear logs which appear at scales much larger than the heavy quark mass. A significant feature of the method is that the perturbative order at which the fixed–order and resummed results are obtained can be chosen independently of each other in the most suitable way: in fact, we have explicitly considered two different NLO implementations (denoted as scheme A and scheme B) in which fixed order results of order α_s or α_s^2 have been combined with NLO parton distributions.

After discussing in detail the method and its implementation to $\mathcal{O}(\alpha_s^2)$, and verifying explicitly its consistency, we have studied the impact of heavy quark corrections and their ambiguity on the F_2 and F_L structure functions. We have found that charm mass effects have a significant impact, at the level of 10% on the charm structure function $F_{2\,c}$ (for fixed PDF) for scales as large as $Q^2 \approx$ 10–20 GeV^2. The effect is rather larger in the threshold region, and also for the $F_{L\,c}$ structure function, for which it is a sizable correction even at $Q^2 \approx 100$ GeV^2. For scales $Q^2 \approx 4$ GeV^2 there is an ambiguity due to subleading terms which are not accurate as threshold, which for $F_{2\,c}$ at $\mathcal{O}(\alpha_s)$ is almost as large as the whole heavy quark correction.

We have seen that introducing a suppression term near threshold for these subleading contributions (such as provided by a damping factor or by so–called χ–scaling) somewhat reduces this ambiguity. Comparison to exact $\mathcal{O}(\alpha_s^2)$ results suggests that this threshold suppression improves the accuracy of the calculation, though beyond these order there are no exact results to compare to. The ambiguity is substantially reduced if $\mathcal{O}(\alpha_s^2)$ heavy quark production terms are used within the NLO computation.

We have finally discussed issues related to mass singularities in the experimental defini-

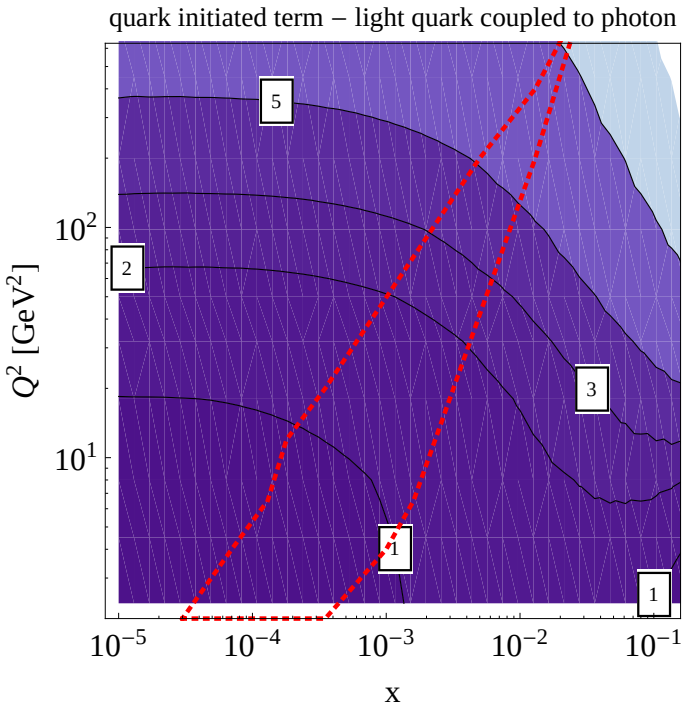

Figure 23: The $\Delta F_{2\,c}^{(n_l)}$ percentage ratio Eq. (83), in the (x, Q^2) plane. The region bounded by the dashed lines is the HERA kinematic range of Fig. 22.

tion of the heavy quark structure functions, which differs somewhat from the theoretically most natural definition: we have seen that the impact of these corrections is small in the HERA kinematic region, but could become relevant at higher energies.

Besides giving a simple, flexible and practically viable implementation of heavy quark effects, our results provide a framework for the understanding of the impact of heavy quark effects on the determination of parton distributions and of the dependence of results on details of the procedure due to its theoretical uncertainties.

Acknowledgements: We thank Andrea Piccione for collaboration in the early stages of this work. We thank Jack Smith for correspondence, and providing computer programs. We are especially grateful to Massimo Corradi for eliciting our interest in issues related to the experimental definition of $F_{2\,c}$ and for continuous assistance with the HVQDIS code. We thank Matteo Cacciari, Joey Huston, Pavel Nadolsky, Fred Olness and Robert Thorne for several useful discussions, and Sergey Alekhin and Johannes Blümlein for clarifications about Ref. [19]. This work was partly supported by the European network HEPTOOLS under contract MRTN-CT-2006-035505 and by the Netherlands Foundation for Fundamental Research of Matter (FOM) and the National Organization for Scientific Research (NWO).

A Appendix: Implementation of the FONLL scheme for $F_2(x,Q^2)$ up to $\mathcal{O}\left(\alpha_s^2\right)$.

In this appendix, we collect the relevant explicit formulae for the practical computation of the the DIS structure function $F_2(x,Q^2)$ within the FONLL approach up to $\mathcal{O}\left(\alpha_s^2\right)$, which has been already discussed more formally in Sec. 3.2.2. Formulae for $F_L(x,Q^2)$ are simpler and can be obtained in an analogous way, and thus are not discussed here. Unlike the formulae found in Sec. 3, given for the purpose of illustration, here we focus on practical implementation issues, i.e., we state which equations and computer codes we have used to arrive to the numerical results for the FONLL structure functions that have been presented in Sec. 4.

For simplicity, we denote in this Appendix F_2 by F and similarly for all the various coefficients, and we write throughout

$$\alpha_s \equiv \alpha_s^{(n_l+1)}(Q^2), \qquad f_i(y,Q^2) = f_i^{(n_l+1)}(y,Q^2)\ . \tag{87}$$

As has been discussed in Sec. 3.2, in order to obtain the full structure function F we compute separately the "light" F_l and "heavy" F_h contributions. For F_h, up to order $\mathcal{O}(\alpha_s^2)$, the relevant equations are

$$\begin{aligned}
F_h^{\rm FONLL}(x,Q^2) &= F_h^{(d)}(x,Q^2) + F_h^{(n_l)}(x,Q^2), &(88)\\
F_h^{(d)}(x,Q^2) &= F_h^{(n_l+1)}(x,Q^2) - F_h^{(n_l,0)}(x,Q^2), &(89)\\
F_h^{(n_l)}(x,Q^2) &= x\sum_{i=g,q,\bar q}\int_{x_\chi}^1 \frac{dy}{y} C_{i,h}^{(n_l)}\left(\frac{x}{y},\frac{Q^2}{m^2},\alpha_s\right) f_i(y,Q^2), &(90)\\
F_h^{(n_l,0)}(x,Q^2) &= x\sum_{i=g,q,\bar q}\int_{x}^1 \frac{dy}{y} C_{i,h}^{(n_l,0)}\left(\frac{x}{y},L,\alpha_s\right) f_i(y,Q^2) &(91)\\
F_h^{(n_l+1)}(x,Q^2) &= x\sum_{i=g,q,\bar q,h,\bar h}\int_{x}^1 \frac{dy}{y} C_{i,h}^{(n_l+1)}\left(\frac{x}{y},\alpha_s\right) f_i(y,Q^2), &(92)
\end{aligned}$$

where $x_\chi = x(1+4m^2/Q^2)$ and $C_{i,h}^{(n_l,0)}$ are the massless limit of the massive coefficient functions $C_{i,h}^{(n_l)}$. Note that in Eqs. (88-92) the PDFs and the strong coupling are always given in the n_l+1 flavour scheme.

Up to $\mathcal{O}(\alpha_s^2)$, the massive coefficient functions $C_{i,h}^{(n_l)}$ are given by

$$\begin{aligned}
zC_{i,h}^{(n_l)}\left(z,\frac{Q^2}{m^2}\right) &= \frac{e_h^2\alpha_s}{(2\pi)^2}\frac{Q^2}{m^2}\Bigg[c_{2,\,i}^{(0)}\left(z,\frac{Q^2}{m^2}\right)\\
&+ 4\pi\alpha_s\left\{c_{2,\,i}^{(1)}\left(z,\frac{Q^2}{m^2}\right) + \bar c_{2,\,i}^{(1)}\left(z,\frac{Q^2}{m^2}\right)\log\frac{Q^2}{m^2}\right\}\Bigg], \qquad (93)
\end{aligned}$$

The massive coefficient functions $c_{2,\,g}^{(1)}$, $\bar c_{2,\,g}^{(1)}$, $c_{2,\,q}^{(1)}$, $\bar c_{2,\,q}^{(1)}$ were first computed in [21], together with the analog expressions for F_L. They are given as phase-space integrals of differential cross sections; the corresponding $c_T^{(1)}$, $c_L^{(1)}$ coefficients (as defined in Ref. [21]) are plotted

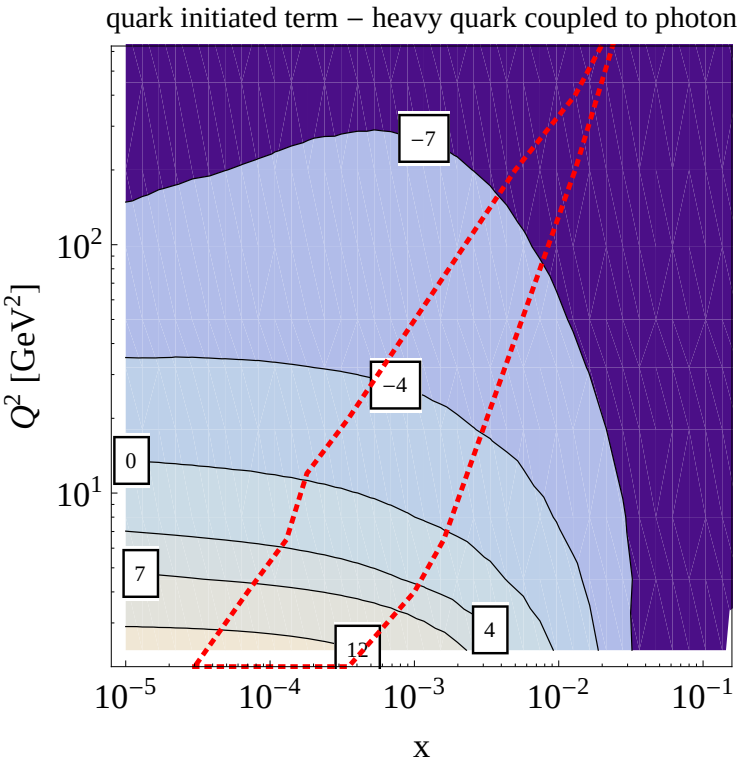

Figure 24: Same as Fig. 23, but for the percentage contribution $R_{\rm light}$ of light-quark initiated terms to $F_{2\,c}$ Eq. (84).

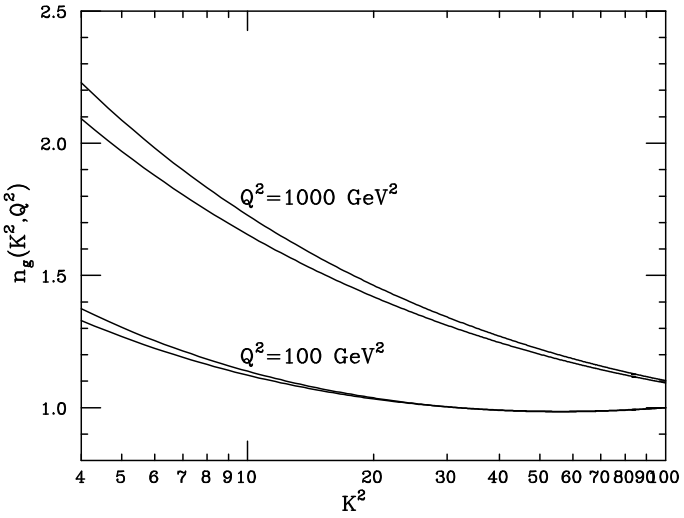

Figure 25: The resummation factor $n_g(Q^2, K^2)$ as a function of K^2, for two values of Q^2. Upper lines have $\Lambda = 300$ MeV, lower lines have $\Lambda = 200$ MeV.

in Figs. 6–10 of that reference (the quark coefficient has been subsequently corrected as Fig. 6 of Ref. [51]). For the FONLL phenomenological studies of Sec. 4 we have used direct numerical integration of the expressions of Ref. [21], benchmarked against the plots in Refs. [21] and [56]; we have not relied upon the interpolation provided in Ref. [57]. The massless–limit expressions of the $C_{i,h}^{(n_l),1}$ coefficients, needed to compute $C_{i,h}^{(n_l,0)}$, were taken from a Fortran implementation [58] of the results of Ref. [32]; they were tested at large values of Q^2 against our massive expressions. The $\overline{\rm MS}$ cross sections $F_h^{(n_l+1)}$ at the NNLO order were computed using the `QCDNUM` program [39].

For the "light" contribution F_l instead, up to order $\mathcal{O}(\alpha_s^2)$, it is convenient to rearrange the expression Eq. (65) of Sec. 3.2.2, exploiting the fact that all contributions to $F^{(d)}$ Eq. (67) cancel except the heavy quark contribution, and that the massive–scheme contribution with n_l flavours is most easily obtained by writing it in terms of the corresponding contribution with n_l+1, which can then be obtained from the `QCDNUM` code. We thus wind up with the following expression:

$$
\begin{aligned}
F_l^{\rm FONLL}(x,Q^2) &= F_l^{(d)} + F_l^{(n_l)}, && (94)\\
F_l^{(d)}(x,Q^2) &= x\sum_{i=h,\bar h}\int_x^1 \frac{dy}{y} C_{i,l}^{(n_l+1)}\left(\frac{x}{y},\alpha_s\right) f_i(y,Q^2), && (95)\\
F_l^{(n_l)}(x,Q^2) &= F_l^{(n_l+1)} - x\sum_{i=h,\bar h}\int_x^1 \frac{dy}{y} C_{i}^{(n_l+1)}\left(\frac{x}{y},\alpha_s\right) f_i(y,Q^2) && (96)\\
&+ x\sum_{i\neq h,\bar h,g}\int_x^1 \frac{dy}{y} D_{i,l}\left(\frac{x}{y},\frac{Q^2}{m^2},\alpha_s\right) f_i(y,Q^2)
\end{aligned}
$$

where we have defined

$$
\begin{aligned}
D_{i,l}\left(z,\frac{Q^2}{m^2},\alpha_s\right) &= \left(\frac{\alpha_s}{4\pi}\right)^2 e_i^2\left[L_q^{(2)}\left(z,\frac{Q^2}{m^2}\right) - \delta(1-z)\int_0^1 dz L_q^{(2)}\left(z,\frac{Q^2}{m^2}\right)\right] && (97)\\
&- \left(\frac{\alpha_s}{2\pi}\right)^2\left[e_i^2 K_{qq}(z,L) + \frac{2T_R}{3} L C_i^{(n_l),1}(z)\right] - \frac{\partial}{\partial n_l} C_i^{(n_l+1)}(z,\alpha_s)
\end{aligned}
$$

where the function $L_q^{(2)}$ is given in formula (A.1) of Ref. [32], with the further assumption

$$
L_q^{(2)}\left(z,\frac{Q^2}{m^2},\alpha_s\right) = 0 \qquad \text{for} \quad z \geq \frac{1}{1+\frac{4m^2}{Q^2}}\,. \tag{98}
$$

The function K_{qq} is given by

$$
\begin{aligned}
K_{qq}(z,L) &= K_{qq}(z) + \frac{L^2}{2}\frac{2T_R}{3} P_{qq}^{((n_l),0)}(z) - L\Delta_{qq}(z), && (99)\\
K_{qq}(z) &= C_F T_R\left[\frac{1+z^2}{1-z}\left(\frac{1}{6}\log^2 z + \frac{5}{9}\log z + \frac{28}{27}\right) + (1-z)\left(\frac{2}{3}\log z + \frac{13}{9}\right)\right]_+ && (100)\\
\Delta_{qq}(z) &= C_F T_R\left[\frac{1+z^2}{1-z}\left(\frac{2}{3}\log z + \frac{10}{9}\right) + \frac{4}{3}(1-z)\right]_+, && (101)
\end{aligned}
$$

and the NLO quark coefficient function (see for example Ref. [59]) is

$$C_i^{(n_l),1} = e_i^2 C_F \left[\frac{1+z^2}{1-z} \left(\log \frac{1-z}{z} - \frac{3}{4} \right) + \frac{1}{4}(9+5z) \right]_+ . \tag{102}$$

The term proportional to $\delta(1-z)$ in Eq. (97) is the heavy flavour virtual correction, and it is needed to enforce the Adler sum rule, which thus determines its coefficient. We can easily see that

$$D_{i,l}\left(\frac{x}{y}, \frac{Q^2}{m^2}, \alpha_s\right) = B_{i,l}\left(\frac{x}{y}, \frac{Q^2}{m^2}, \alpha_s\right) - C_i^{(n_l+1)}\left(\frac{x}{y}, \alpha_s\right), \tag{103}$$

so that, using also Eq. (63), we have

$$F_l^{(n_l)} = x \sum_{i \neq h,\bar{h}} \int_x^1 \frac{dy}{y} B_{i,l}\left(\frac{x}{y}, \frac{Q^2}{m^2}, \alpha_s\right) f_i(y, Q^2). \tag{104}$$

In Eq. (96), the term $F_l^{(n_l+1)}$ is evaluated directly using the `QCDNUM` program. All remaining terms must be evaluated independently. Note that the second term on the r.h.s of Eq. (96) is identical to Eq. (95): these terms thus would cancel exactly, but the cancellation does not happen if one uses a threshold prescription such as Eq. (19) or Eq. (20), because the threshold prescription only affects $F^{(d)}$ but not $F^{(n_l)}$. The coefficients of n_l in $C_i^{(n_l+1)}$ and $C_{h/\bar{h},l}^{(n_l+1)}$ have been evaluated using the same equations as the `QCDNUM` package, given in Refs. [60] and [61], since they have to compensate the `QCDNUM` result in $F_l^{(n_l+1)}$. Notice that, according to Eq. (71) $D_{i,l}$ vanishes in the massless limit.

All the $\mathcal{O}(\alpha_s^2)$ results given so far, used with NNLO PDFs, correspond to the scheme C of Sec. 3.3. The $\mathcal{O}(\alpha_s)$ results (scheme A) were obtained using the same formulae, truncated at order α_s, and using NLO evolution and massless coefficient functions in `QCDNUM`. The alternative NLO implementation, denoted by scheme B in Sec. 3.3, uses the NLO approximation in the massless result, and the full $\mathcal{O}(\alpha_s^2)$ result in the massive one is also obtained in a similar way. The only caveat is that in the subtracted term in Eq. (91) we replace the massless limit of the $C_{g,h}^{(n_l),1}$ (denoted by $C_{g,h}^{(n_l,0),1}$) with

$$C_{g,h}^{(n_l,0),1}\left(z, \frac{Q^2}{m^2}\right) \to C_{g,h}^{(n_l,0),1}\left(z, \frac{Q^2}{m^2}\right) - C_{g,h}^{(n_l,0),1}(z,1), \tag{105}$$

i.e. the non-logarithmic term is excluded from the subtraction, according to the discussion in Sec. 2.2.

References

[1] W. K. Tung, H. L. Lai, A. Belyaev, J. Pumplin, D. Stump and C. P. Yuan, JHEP **0702** (2007) 053 [arXiv:hep-ph/0611254].

[2] J. C. Collins, Phys. Rev. D **58** (1998) 094002 [arXiv:hep-ph/9806259].

[3] M. A. G. Aivazis, J. C. Collins, F. I. Olness and W. K. Tung, Phys. Rev. D **50** (1994) 3102 [arXiv:hep-ph/9312319].

[4] J. C. Collins, F. Wilczek and A. Zee, Phys. Rev. D **18** (1978) 242.

[5] M. 1. Kramer, F. I. Olness and D. E. Soper, Phys. Rev. D **62** (2000) 096007 [arXiv:hep-ph/0003035].

[6] W. K. Tung, S. Kretzer and C. Schmidt, J. Phys. G **28** (2002) 983 [arXiv:hep-ph/0110247].

[7] S. Kretzer, H. L. Lai, F. I. Olness and W. K. Tung, Phys. Rev. D **69** (2004) 114005 [arXiv:hep-ph/0307022].

[8] R. S. Thorne and R. G. Roberts, Phys. Rev. D **57** (1998) 6871 [arXiv:hep-ph/9709442].

[9] R. S. Thorne and R. G. Roberts, Phys. Lett. B **421** (1998) 303 [arXiv:hep-ph/9711223].

[10] R. S. Thorne, Phys. Rev. D **73** (2006) 054019 [arXiv:hep-ph/0601245].

[11] A. D. Martin, R. G. Roberts, W. J. Stirling and R. S. Thorne, Eur. Phys. J. C **4** (1998) 463 [arXiv:hep-ph/9803445].

[12] A. D. Martin, R. G. Roberts, W. J. Stirling and R. S. Thorne, Eur. Phys. J. C **23** (2002) 73 [arXiv:hep-ph/0110215].

[13] A. D. Martin, R. G. Roberts, W. J. Stirling and R. S. Thorne, Eur. Phys. J. C **28** (2003) 455 [arXiv:hep-ph/0211080].

[14] A. D. Martin, W. J. Stirling, R. S. Thorne and G. Watt, Eur. Phys. J. C **63** (2009) 189 [arXiv:0901.0002 [hep-ph]].

[15] R. S. Thorne and W. K. Tung, arXiv:0809.0714 [hep-ph].

[16] F. Olness and I. Schienbein, Nucl. Phys. Proc. Suppl. **191** (2009) 44 [arXiv:0812.3371 [hep-ph]].

[17] M. Cacciari, M. Greco and P. Nason, JHEP **9805** (1998) 007 [arXiv:hep-ph/9803400].

[18] M. Buza, Y. Matiounine, J. Smith and W. L. van Neerven, Eur. Phys. J. C **1** (1998) 301 [arXiv:hep-ph/9612398].

[19] S. Alekhin, J. Blumlein, S. Klein and S. Moch, Phys. Rev. D **81** (2010) 014032 [arXiv:0908.2766 [hep-ph]].

[20] S. Alekhin, J. Blumlein, S. Klein and S. Moch, *private communication.*

[21] E. Laenen, S. Riemersma, J. Smith and W. L. van Neerven, Nucl. Phys. B **392** (1993) 162.

[22] S. J. Brodsky, C. Peterson and N. Sakai, Phys. Rev. D **23** (1981) 2745.

[23] J. Pumplin, H. L. Lai and W. K. Tung, Phys. Rev. D **75** (2007) 054029 [arXiv:hep-ph/0701220].

[24] M. Buza, Y. Matiounine, J. Smith and W. L. van Neerven, Phys. Lett. B **411** (1997) 211 [arXiv:hep-ph/9707263].

[25] P. Nadolsky, *private communication*.

[26] P. M. Nadolsky and W. K. Tung, Phys. Rev. D **79** (2009) 113014 [arXiv:0903.2667 [hep-ph]].

[27] E. G. Floratos, D. A. Ross and C. T. Sachrajda, Nucl. Phys. B **152** (1979) 493.
W. Furmanski and R. Petronzio, Phys. Lett. B **97** (1980) 437.
E. G. Floratos, C. Kounnas and R. Lacaze, Nucl. Phys. B **192** (1981) 417.

[28] J. A. M. Vermaseren, A. Vogt and S. Moch, Nucl. Phys. B **724** (2005) 3 [arXiv:hep-ph/0504242].

[29] W. L. van Neerven and E. B. Zijlstra, Phys. Lett. B **272** (1991) 127.

[30] E. B. Zijlstra and W. L. van Neerven, Phys. Lett. B **273** (1991) 476.

[31] E. B. Zijlstra and W. L. van Neerven, Nucl. Phys. B **383** (1992) 525.

[32] M. Buza, Y. Matiounine, J. Smith, R. Migneron and W. L. van Neerven, Nucl. Phys. B **472** (1996) 611 [arXiv:hep-ph/9601302].

[33] M. Buza and W. L. van Neerven, Nucl. Phys. B **500** (1997) 301 [arXiv:hep-ph/9702242].

[34] G. Corcella and A. D. Mitov, Nucl. Phys. B **676** (2004) 346 [arXiv:hep-ph/0308105].

[35] I. Bierenbaum, J. Blumlein and S. Klein, Nucl. Phys. B **820** (2009) 417 [arXiv:0904.3563 [hep-ph]].

[36] J. Rojo *et al.*, Sect. III/22 in T. Binoth *et al.*, arXiv:1003.1241 [hep-ph].

[37] A. Chuvakin, J. Smith and W. L. van Neerven, Phys. Rev. D **61** (2000) 096004 [arXiv:hep-ph/9910250].

[38] W. Giele *et al.*, arXiv:hep-ph/0204316.

[39] M. Botje, `http://www.nikhef.nl/ h24/qcdnum/`

[40] M. Dittmar *et al.*, arXiv:hep-ph/0511119.

[41] S. Catani, M. Ciafaloni and F. Hautmann, Nucl. Phys. B **366** (1991) 135.

[42] *Preprint* H1prelim-09-171, ZEUS-prelim-09-015 (October 2009);
M. Corradi, *private communication*.

[43] J. Breitweg *et al.* [ZEUS Collaboration], Eur. Phys. J. C **12** (2000) 35 [arXiv:hep-ex/9908012].

[44] C. Adloff *et al.* [H1 Collaboration], Phys. Lett. B **528** (2002) 199 [arXiv:hep-ex/0108039].

[45] A. Aktas *et al.* [H1 Collaboration], Eur. Phys. J. C **40** (2005) 349 [arXiv:hep-ex/0411046].

[46] A. Aktas *et al.* [H1 Collaboration], Eur. Phys. J. C **45** (2006) 23 [arXiv:hep-ex/0507081].

[47] A. Aktas *et al.* [H1 Collaboration], Eur. Phys. J. C **51** (2007) 271 [arXiv:hep-ex/0701023].

[48] S. Chekanov *et al.* [ZEUS Collaboration], Eur. Phys. J. C **63**

[49] S. Chekanov *et al.* [ZEUS Collaboration], arXiv:0904.3487 [hep-ex].

[50] F. D. Aaron *et al.* [H1 Collaboration], arXiv:0907.2643 [hep-ex].

[51] B. W. Harris and J. Smith, Nucl. Phys. B **452**, 109 (1995) [arXiv:hep-ph/9503484].

[52] S. Chekanov *et al.* [ZEUS Collaboration], Phys. Rev. D **67** (2003) 012007 [arXiv:hep-ex/0208023].

[53] J. B. Dainton, M. Klein, P. Newman, E. Perez and F. Willeke, JINST **1** (2006) P10001 [arXiv:hep-ex/0603016].

[54] M. L. Mangano and P. Nason, Phys. Lett. B **285** (1992) 160.

[55] A. H. Mueller and P. Nason, Nucl. Phys. B **266** (1986) 265.

[56] B.W. Harris and J. Smith, Phys. Rev. D57 (1998) 2806, hep-ph/9706334.

[57] S. Riemersma, J. Smith and W. L. van Neerven, Phys. Lett. B **347** (1995) 143 [arXiv:hep-ph/9411431].

[58] J. Smith, *private communication*

[59] W. Furmanski and R. Petronzio, Z. Phys. C **11** (1982) 293.

[60] W. L. van Neerven and A. Vogt, Nucl. Phys. B **568** (2000) 263 [arXiv:hep-ph/9907472].

[61] W. L. van Neerven and A. Vogt, Nucl. Phys. B **588** (2000) 345 [arXiv:hep-ph/0006154].